Supplementary Information (SI) for Journal of Materials Chemistry A.
This journal is © The Royal Society of Chemistry 2024

Supplementary Information

Recycle of organic ligands and solvents for successive synthesis of Cu-based nanocrystals towards CO_2 hydrogenation

Yue Xin[a,1], Zicheng Xie[a,1], Rui Liu[a], Qi Li[a], Zheng Wang[a], Dongqiang Cao[a], Shuhui Li[a], Lantian Zhang[a], Sunpei Hu[b], Hongliang Li[b], Rong He[d], Liangbing Wang[a,*], and Jie Zeng[b,c,*]

[a] State Key Laboratory for Powder Metallurgy, School of Materials Science and Engineering, Central South University, Changsha, Hunan 410083, P. R. China

[b] Hefei National Research Center for Physical Sciences at the Microscale, Key Laboratory of Strongly-Coupled Quantum Matter Physics of Chinese Academy of Sciences, National Synchrotron Radiation Laboratory, Key Laboratory of Surface and Interface Chemistry and Energy Catalysis of Anhui Higher Education Institutes, Department of Chemical Physics, University of Science and Technology of China, Hefei, Anhui 230026, P. R. China

[c] School of Chemistry and Chemical Engineering, Anhui University of Technology, Ma'anshan, Anhui 243002, P. R. China

[d] State Key Laboratory of Environment-friendly Energy Materials, National Co-innovation Center for Nuclear Waste Disposal and Environmental Safety, Sichuan Institute of Military and Civilian Integration, Nuclear Waste and Environmental Safety Key Laboratory of Defense, School of Life Science and Engineering, Joint Laboratory for Extreme Conditions Matter Properties, Southwest University of Science and Technology, 621010 Mianyang, Sichuan, P. R. China

* Corresponding authors: wanglb@csu.edu.cn; zengj@ustc.edu.cn

[1] These authors contributed equally to this work.

Experimental sections

1. Chemicals and materials. Copper sulfate pentahydrate ($CuSO_4·5H_2O$, ≥99%), sodium hydroxide (NaOH, ≥96.0%), ferric chloride hexahydrate ($FeCl_3·6H_2O$, ≥99%), cobalt chloride hexahydrate ($CoCl_2·6H_2O$, ≥99%), nickel chloride hexahydrate ($NiCl_2·6H_2O$, 99%), zirconyl chloride octahydrate ($ZrOCl_2·8H_2O$, 98%), zinc chloride ($ZnCl_2$, 98%), cerium(III) chloride heptahydrate ($CeCl_3·7H_2O$, 99%), and manganese sulfate monohydrate ($MnSO_4·H_2O$, 99%) were obtained from Sinopharm Chemical Reagent Co., Ltd. Acetylacetone ($C_5H_8O_2$, Hacac, 99%), all the commercial metal acetylacetonate, methanol (CH_3OH, HPLC), and hexane (C_6H_{14}, 97%) were purchased from Shanghai Macklin Biochemical Co., Ltd. 1-octadecene ($C_{18}H_{36}$, 90%), oleic acid ($C_{18}H_{34}O_2$, AR), oleylamine ($C_{18}H_{37}N$, 80%-90%), and octadecanol ($C_{18}H_{38}O$, 99%) were obtained from Shanghai Aladdin Biochemical Technology Co., Ltd. High purity nitrogen (N_2, ≥99.999%), $H_2/CO_2/N_2$ mixed gas ($H_2/CO_2/N_2$ = 72/24/4, N_2 as the internal standard), and H_2/Ar mixed gas (H_2/Ar = 1/9) were purchased from Saizhong Special Gas Co., Ltd in Changsha. All chemical reagents were used as received without further purification. All aqueous solutions were prepared using ultrapure water with a resistivity of 18.2 $M\Omega·cm^{-1}$.

2. Fabrication of CuO NCs and recovery of organic ligands, synthesis, and purification solvents

2.1 Synthesis of $Cu(acac)_2$ from $CuSO_4 \cdot 5H_2O$. The preparation of $Cu(acac)_2$ was via the liquid phase method using $CuSO_4 \cdot 5H_2O$ and the organic ligand Hacac (**Figure S1**). In a typical synthesis of $Cu(acac)_2$ with a target mass of 50 g, 47.75 g of $CuSO_4 \cdot 5H_2O$ was firstly dissolved in 200 mL of ultrapure water in a 500-mL flask under magnetic stirring for 10 min to form a homogeneous solution. 41 mL of Hacac was then added into the mixture under stirring in an ice bath for 30 min, during which Hacac chelated with Cu^{2+} to form $Cu(acac)_2$:

$$CuSO_4 \cdot 5H_2O + 2Hacac \rightarrow Cu(acac)_2 + H_2SO_4 + 5H_2O$$

Subsequently, 100 mL of NaOH (3.82 M) was injected into the mixture at a rate of 3 $mL \cdot min^{-1}$ under stirring in an ice bath to neutralize the generated H_2SO_4. The gathered $Cu(acac)_2$ was further immersed in ultrapure water for 30 min in an ice bath to remove the generated Na_2SO_4, which was then washed and collected via the vacuum suction filter system. This process was repeated three times to remove the impurities. The washed $Cu(acac)_2$ powder was finally dried at 80 °C under vacuum for 12 h.

Detection of $Cu(acac)_2$ via high performance liquid chromatography (HPLC) for the determination of the purity and yield of home-made $Cu(acac)_2$. During the detection of $Cu(acac)_2$, HPLC was carried out on a Shimadzu C18 column (150 mm) with methanol as the mobile phase. The column temperature, flow rate, and detection wavelength were set as 40 °C, 0.3 $ml \cdot min^{-1}$, and 293 nm, respectively. To calibrate the concentration-area curve, 0.5 mL of standard methanol solutions of commercial $Cu(acac)_2$ with the concentrations of 0, 100, 150, 200, and 250 $mg \cdot L^{-1}$ were injected into HPLC through the 20-μL quantitative injection loop to achieve standard analyte peaks for $Cu(acac)_2$. The retention time of $Cu(acac)_2$ was about 3.4 min. The profile of peak areas versus the concentrations of standard solutions was plotted, where a linear correlation with $R^2 = 0.999$ was obtained (**Figure S2a**). The purity of the home-made $Cu(acac)_2$ was determined by HPLC in comparison with commercial $Cu(acac)_2$. To determine the purity of home-made $Cu(acac)_2$, 10 mg of home-made $Cu(acac)_2$ was fixed to the volume with methanol via a 50-

mL volumetric flask to achieve a concentration of approximately 200 mg·L^{-1}. The Cu(acac)$_2$ solution was then analyzed by using the same method. According to the peak areas and standard curve, the actual concentration of the Cu(acac)$_2$ solution was obtained. Thus, the purity of home-made Cu(acac)$_2$ was determined via the following equation:

$$P_{Cu(acac)2} = \frac{C_{Cu(acac)2,a}}{C_{Cu(acac)2}} \times 100\%$$

where $C_{Cu(acac)2,a}$ and $C_{Cu(acac)2}$ represented the actual concentration of the Cu(acac)$_2$ solution detected via HPLC and the theoretical concentration of the Cu(acac)$_2$ solution, respectively. The ultimate yield of home-made Cu(acac)$_2$ ($Y_{Cu(acac)2}$) was calculated based on the following equation:

$$Y_{Cu(acac)2} = \frac{m_{Cu(acac)2} \times P_{Cu(acac)2}}{m_{Cu(acac)2,t}} \times 100\%$$

where $m_{Cu(acac)2}$ and $m_{Cu(acac)2,t}$ were the actual and target mass of produced Cu(acac)$_2$, respectively. In this work, $C_{Cu(acac)2,a}$ was determined as 196.9 mg·L^{-1} via HPLC, thus:

$$P_{Cu(acac)2} = \frac{C_{Cu(acac)2,a}}{C_{Cu(acac)2}} \times 100\% = \frac{196.9\ mg \cdot L^{-1}}{200.0\ mg \cdot L^{-1}} \times 100\% = 98.5\%$$

$m_{Cu(acac)2}$ and $m_{Cu(acac)2,t}$ were 49.93 and 50 g, respectively, thus:

$$Y_{Cu(acac)2} = \frac{m_{Cu(acac)2} \times P_{Cu(acac)2}}{m_{Cu(acac)2,t}} \times 100\% = \frac{49.93\ g \times 98.5\%}{50\ g} \times 100\% = 98.4\%$$

Detection of components in soaking liquid and filtrates. The soaking liquid and filtrates during the synthesis of Cu(acac)$_2$ were gathered to further detect the amount of Hacac and Cu species in them via HPLC and inductively coupled plasma-atomic emission spectrometry (ICP-AES), respectively. The main components of the filtrates were Hacac and Cu(acac)$_2$ that were able to be recycled. Nevertheless, a small amount of Cu(acac)$_2$ and Hacac in the soaking liquid was considered as the loss during synthetic process due to the co-existence of a mass of generated Na_2SO_4. The utilization efficiency of Hacac during the synthesis of Cu(acac)$_2$ ($U_{Hacac,Cu}$) was calculated in terms of the following equation:

$$U_{Hacac,Cu} = \frac{m_{Cu(acac)2} \times P_{Cu(acac)2} \times V_{Hacac} \times 2}{M_{Cu(acac)2} \times v_{Hacac,Cu}} \times 100\%$$

where $M_{Cu(acac)2}$, V_{Hacac}, and $v_{Hacac,Cu}$ were the molar mass of $Cu(acac)_2$, the molar volume of Hacac, and the volume of Hacac used in the synthesis of $Cu(acac)_2$, respectively. For this work:

$$U_{Hacac,Cu} = \frac{m_{Cu(acac)2} \times P_{Cu(acac)2} \times V_{Hacac} \times 2}{M_{Cu(acac)2} \times v_{Hacac,Cu}} \times 100\% = \frac{49.93\ g \times 98.5\%}{261.76\ g} = 96.5\%$$

For the detection of Hacac, HPLC was carried out on a Shimadzu C18 column (150 mm) with methanol as the mobile phase. The column temperature, flow rate, and detection wavelength were set as 40 °C, 0.3 ml·min^{-1}, and 273 nm, respectively. To calibrate the concentration-area curve, 0.5 mL of standard methanol solutions of Hacac with the concentrations of 0, 0.01, 0.05, 0.1, 0.15, 0.2, and 0.25 mL·L^{-1} were injected into HPLC through the 20-μL quantitative injection loop to achieve standard analyte peaks for Hacac. The retention time of Hacac was about 5.6 min. The profile of peak areas versus the concentrations of standard solution was plotted, where a linear correlation with $R^2 = 0.999$ was obtained (**Figure S2b**). The amount of Hacac in the soaking liquid and filtrates was quantified according to the peak areas and standard curve. In this work, the volumes of filtrates and soaking liquid were 262 and 220 mL, respectively. For the soaking liquid, approximately 0.02 mL of Hacac was detected in it, while the amount of Cu species was below the limit of detection (LOD) of ICP-AES. The volume of Hacac and the mass of Cu species were determined as 0.16 mL and 3.90 mg in filtrates, respectively.

2.2 Fabrication of CuO NCs and recovery of organic ligands, synthesis, and purification solvents

Standard fabrication of CuO NCs and recovery of solvents. In a typical synthesis of CuO NCs, 120 mL of ODE and 30 mL of OA were mixed together in a four-neck flask and then heated to 260 ℃ under stirring in N_2 gas flow. Subsequently, 30 g of home-made $Cu(acac)_2$ was added into the solution over approximately 20 min through a customized sample injector, after which the mixture was held at 260 ℃ for another 20 min and then cooled to room temperature. A violent

reaction occurred with the generation of large amounts of smoke after adding $Cu(acac)_2$ and the initial transparent solution turned to turbid and brownish black. Cu NCs as products were separated by adding 800 mL of ethanol antisolvent to the reaction solution, followed by centrifugation at 12000 rpm for 20 min. Cu NCs were further calcinated at 500 ℃ for 1 h in air flow (1 bar, 50 sccm) to remove the residual organic solvents, after which CuO NCs were finally obtained. Moreover, a condensate tube and a 250-mL flask with 200 mL of H_2O in it were orderly connected with the four-neck flask to recover the generated Hacac during the synthetic process. The concentration of Hacac was further detected via HPLC. Besides, the collected supernatants were distilled to separate ODE/OA and ethanol using a laboratory rotary evaporator.

Cu NCs before calcination for TEM characterization. Cu NCs before calcination for morphology and structure analysis were further washed with hexane and ethanol to remove excess reactants and byproducts. Typically, 2 mL of hexane and 20 mL of ethanol were added into 0.5 mL of synthesis solution containing Cu NCs, followed by centrifugated at 12000 rpm for 20 min after ultrasonic treatment for 30 min. This process was repeated for several times, and the washed Cu NCs were redispersed in hexane for TEM characterization.

Detection of recovered ODE and ethanol via gas chromatography (GC). The amount of recovered ODE and ethanol was detected via GC (Shimadzu GC-2014C) equipped with a flame ionization detector. To calibrate the concentration-peak area curve, a series of standard ODE and ethanol solutions were prepared. The profiles of peak areas versus the concentrations were then plotted (**Figure S4**).

Calculations of production rate of the generated NCs and recovery rate of solvents. The production rate of the generated NCs was calculated via the following equation:

$$P_{NCs} = \frac{M_{NCs,a}}{M_{NCs,t}} \times 100\%$$

where $M_{NCs,a}$ and $M_{NCs,t}$ were the actual and theoretical masses of generated NCs after calcination, respectively.

The recovery rate of the organic ligand Hacac (R_{Hacac}) was determined based on the following

equation:

$$R_{Hacac} = \frac{V_{Hacac,a}}{V_{Hacac,t}} \times 100\%$$

where $V_{Hacac,a}$ and $V_{Hacac,t}$ were the actual and theoretical amounts of recovered Hacac, respectively.

The recovery rates of synthesis and purification solvents *i* (R_i) were calculated in terms of the following equation:

$$R_i = \frac{V_i}{U_i} \times 100\%$$

where V_i and U_i represented the amount of the recovery solvent *i* and the usage of the solvent *i* during synthetic process, respectively.

2.3 Mechanism study of CuO NCs synthesis and Hacac recovery

Control synthesis of Cu NCs with ODE and recovery of Hacac. The control synthesis of Cu NCs with single ODE was conducted by using the same experimental device as the standard synthesis of Cu NCs. 150 mL of ODE in a 250 mL four-neck flask was heated to 260 ℃ under stirring in the flow of N_2 gas and kept at that temperature for 10 min. 30 g of $Cu(acac)_2$ was then added into the solution within 20 min. After another 20 min at 260 ℃, the reaction solution was cooled to room temperature. The resulting Cu NCs were precipitated from the reaction solution by adding 800 mL of ethanol and being centrifugated at 12000 rpm for 10 min. Hacac was also recovered and detected during control synthesis via the similar method used for the standard synthesis of Cu NCs. In addition, water vapor was also introduced in situ into the ODE solvent during the synthesis of Cu NCs to preliminarily investigate the role of H_2O in Hacac recovery.

Isotope labelling experiment with D_2O via the detection of high-resolution gas chromatography-mass spectrometer (HR GC-MS) measurements. To further verify the hydrogen source of recovered Hacac, the D_2O-labelled test was carried out under similar conditions. ODE was pretreated by $MgSO_4$ drying agent to remove as much residual H_2O as possible. $Cu(acac)_2$ was immersed in D_2O for 24 h and then dried at 80 °C under vacuum for 12 h,

after which $Cu(acac)_2$ containing D_2O (named as $Cu(acac)_2 \cdot xD_2O$) was acquired. For the D_2O-labelled test, 150 mL of dried ODE and 3 mL of D_2O were mixed together in a four-neck flask and heated to 260 ℃ under stirring in N_2 gas flow. 30 g of $Cu(acac)_2 \cdot xD_2O$ was then added into the solution at a rate of approximately 1.5 $g \cdot min^{-1}$ through a sample injector, after which the mixture was held at 260 ℃ for another 20 min before it was cooled to room temperature. A condensate tube and a 200-mL flask were orderly connected with the four-neck flask to gather the generated products. It's worth mentioning that no H_2O was in the 250-mL flask. The gathered solution was further diluted by hexane for the detection via HR GC-MS (ThermoFisher Scientific Com.).

Control reaction with CuO and ODE. A control reaction with CuO and ODE was conducted to elucidate the role of ODE during the synthesis of Cu NCs. 1 g of CuO powder and 10 mL of ODE were mixed together and heated to 260 ℃ under N_2 atmosphere. The mixture was maintained at that temperature for 60 min, followed by being centrifuged at 12000 rpm for 10 min after cooled to room temperature. The obtained powder was gathered for further XRD characterization. Besides, the supernatant after reaction was collected and further detected via ^1H nuclear magnetic resonance (NMR, Bruker AVANCE III 500M). 10 μL of the supernatant was dissolved in 600 μL of $CDCl_3$ for ^1H NMR test.

Control synthesis of Cu NCs with different surfactants. The control synthesis of Cu NCs with different surfactants was performed using the similar procedure to the standard synthesis of Cu NCs, except that 30 mL of OA was adjusted to 30 mL of OAm or ODL. Cu NCs and Hacac were also gathered for further characterizations.

Control synthesis of Cu NCs without N_2 gas. The control synthesis of Cu NCs without N_2 was conducted under the similar conditions to the standard synthesis of Cu NCs, except that no N_2 was introduced during the synthesis process.

Control synthesis of Cu NCs via heating-up method. In a typical synthesis via heating-up method, 30 g of $Cu(acac)_2$, 120 mL of ODE, and 30 mL of OA were added into a 250-mL four-neck flask at room temperature. The mixture was gradually heated to 260 ℃ under stirring in the flow of N_2 gas, and maintained at that temperature for 30 min. After the solution was cooled to

room temperature, the generated Cu NCs were precipitated from the reaction solution by adding 800 mL of ethanol and being centrifugated at 12000 rpm for 10 min.

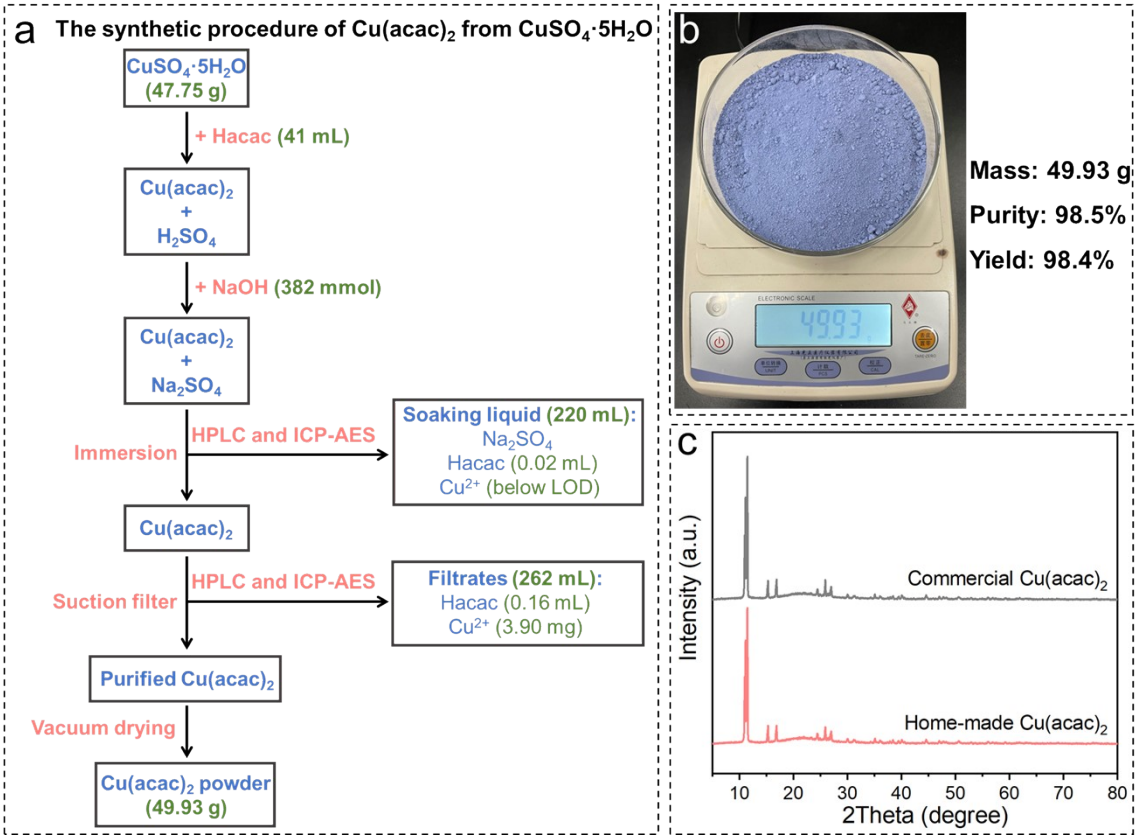

Figure S1. (a) The synthetic procedure of $Cu(acac)_2$ from $CuSO_4 \cdot 5H_2O$. (b) The picture of home-made $Cu(acac)_2$. (c) XRD profiles of home-made and commercial $Cu(acac)_2$.

In a single synthetic process of $Cu(acac)_2$ from $CuSO_4 \cdot 5H_2O$, 49.93 g of $Cu(acac)_2$ was produced with a purity of 98.5% and a yield of 98.4%. Besides, the utilization efficiency of Hacac achieved 96.5%. Only 0.02 mL of Hacac was detected in the soaking liquid, while the amount of Cu species in it was below the LOD of ICP-AES. Only 0.61 mL of Hacac and 3.90 mg of Cu species were determined in filtrates.

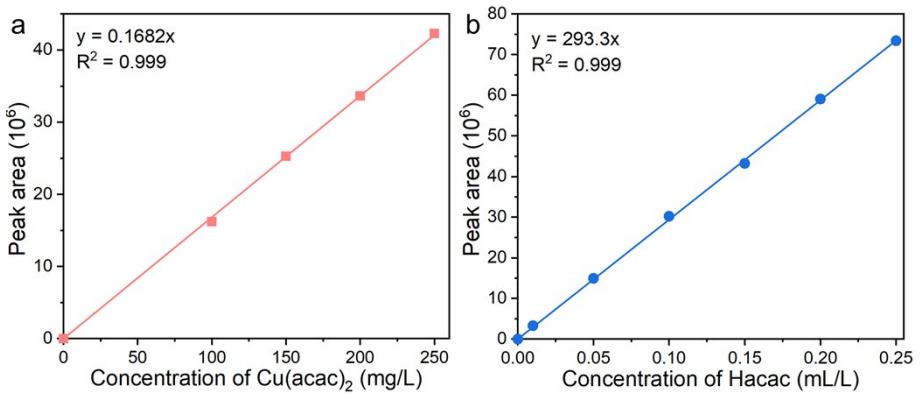

Figure S2. (a-b) Standard curves of the detection of $Cu(acac)_2$ and Hacac via HPLC.

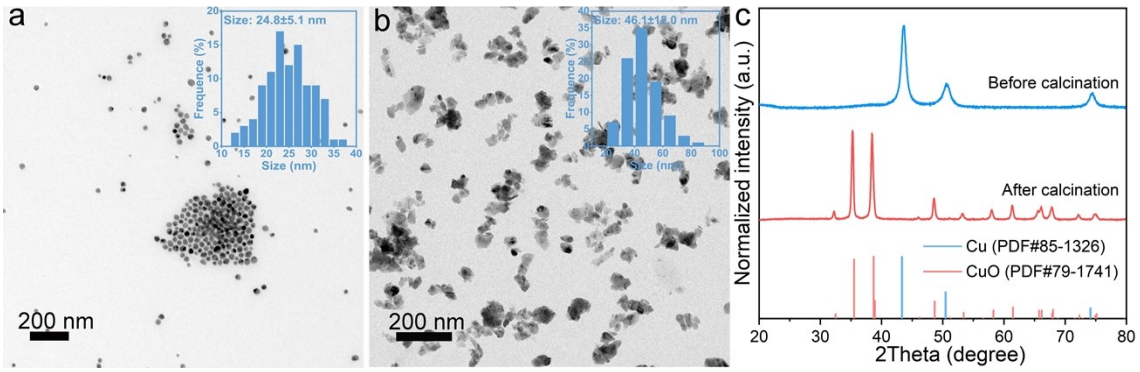

Figure S3. TEM images of Cu NCs (a) before and (b) after calcination. The insets in panels a and b were the size distribution histograms of Cu NCs before and after calcination, respectively. (c) XRD patterns of Cu and CuO NCs.

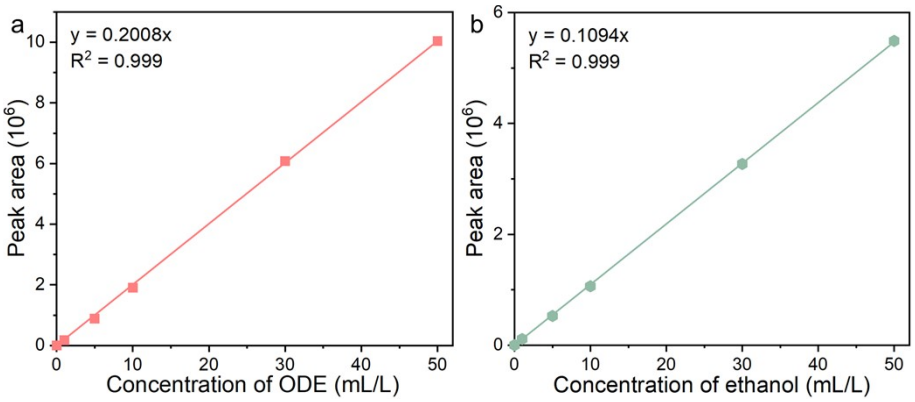

Figure S4. Standard curves of the detection of (a) ODE and (b) ethanol.

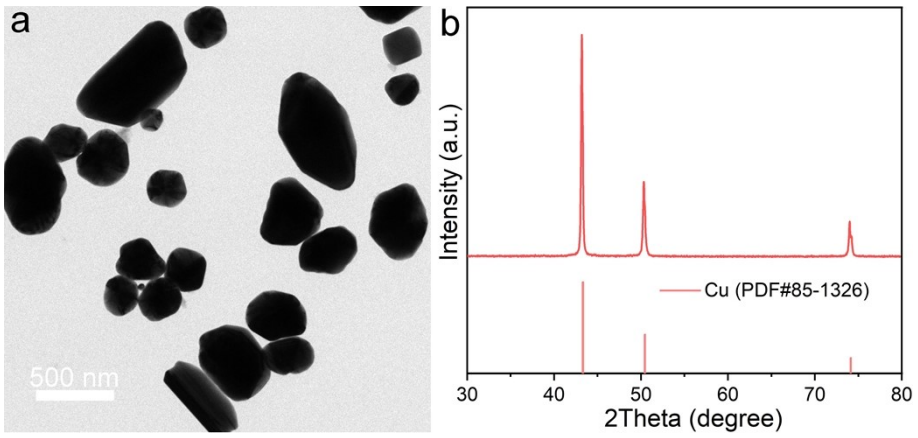

Figure S5. (a) TEM image and (b) XRD pattern of Cu particles synthesized with only ODE as the solvent.

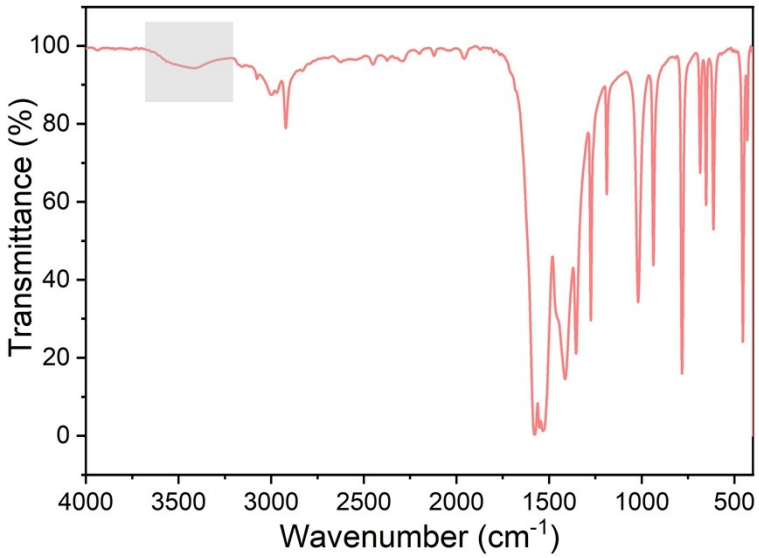

Figure S6. Fourier transform infrared (FTIR) spectra of home-made $Cu(acac)_2$.

The band at around 3443 cm^{-1} indicated the existence of water in home-made $Cu(acac)_2$.[S1]

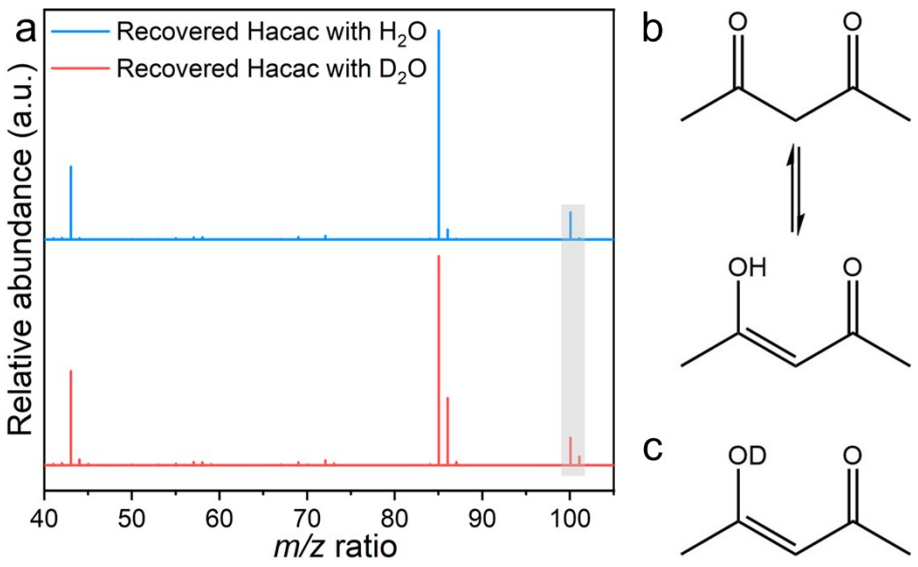

Figure S7. (a) HR GC-MS spectra of the recovered Hacac with H_2O and D_2O. Molecular structures of (b) Hacac and (c) Dacac.

Due to the diketo-enol tautomerization, Hacac generally exists in two forms, i.e. diketo and enol.[S2]

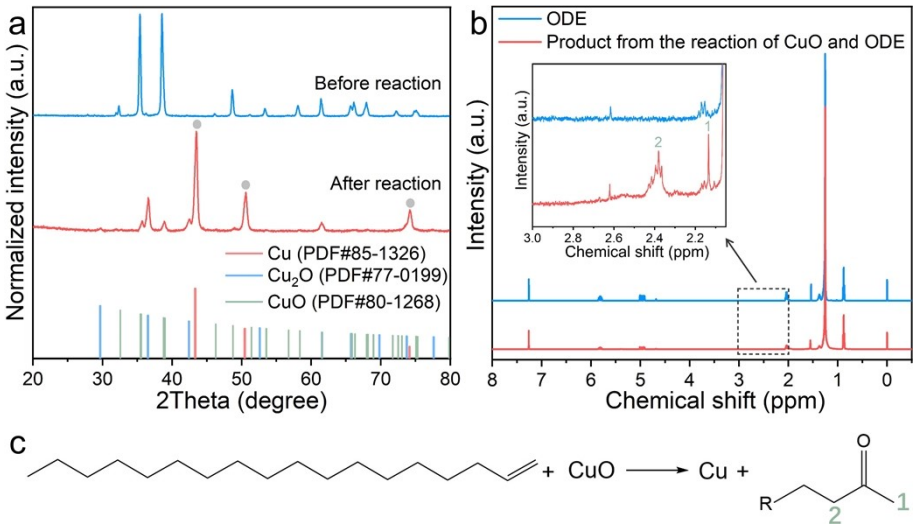

Figure S8. (a) XRD patterns of CuO powders before and after reaction with ODE. (b) ^{1}H NMR spectra of the supernatant from the reaction of CuO and ODE. (c) The proposed reaction between CuO and ODE with the formation of Cu and ketone based on the ^{1}H NMR results.[S3]

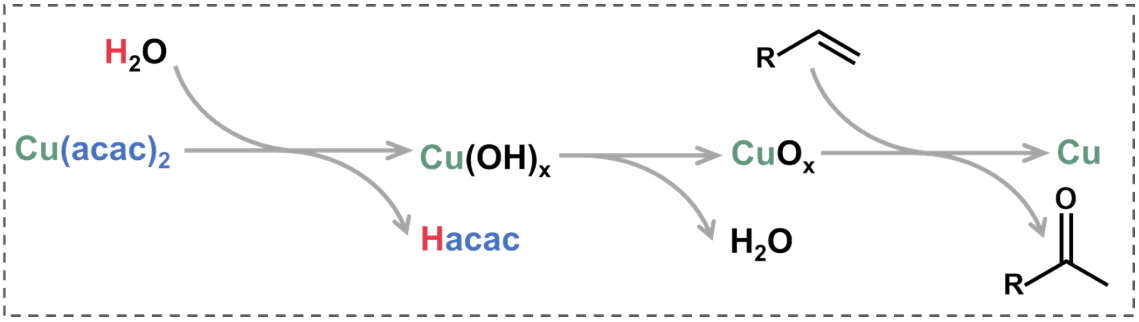

Figure S9. Schematic diagram of the recovery of Hacac and formation of Cu NCs.

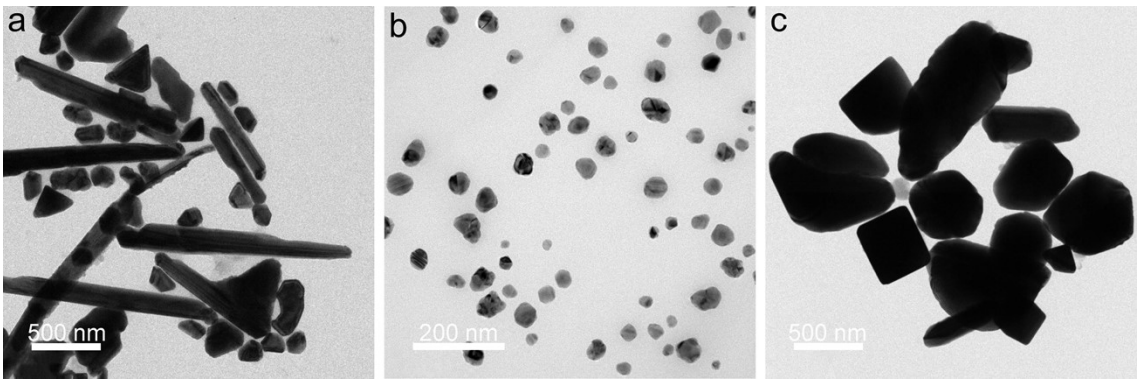

Figure S10. TEM images of Cu NCs synthesized (a) with octadecanol as the surfactant, (b) with OAm as the surfactant, and (c) via the heating-up method.

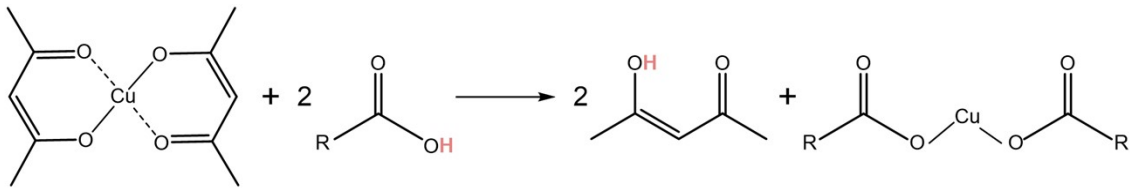

Figure S11. Ligand exchange between OA and $Cu(acac)_2$ with the formation of Hacac.

3. Fabrication of Fe_2O_3 NCs and recovery of organic ligands, synthesis, and purification solvents

3.1 Synthesis of $Fe(acac)_3$ from $FeCl_3 \cdot 6H_2O$. The synthesis of $Fe(acac)_3$ was carried out via the similar liquid phase method. In a typical synthesis of $Fe(acac)_3$ with a target mass of 50 g, 38.27 g of $FeCl_3 \cdot 6H_2O$ was dissolved in 200 mL of ultrapure water in a 500-mL flask under magnetic stirring for 10 min to form a homogeneous solution. 45 mL of Hacac was then added into the flask under stirring in an ice bath for 30 min, during which Hacac chelated with Fe^{3+} to form $Fe(acac)_3$:

$$FeCl_3 \cdot 6H_2O + 3Hacac \rightarrow Fe(acac)_3 + 3HCl + 6H_2O$$

100 mL of NaOH (4.25 M) was injected into the mixture at a rate of 3 $mL \cdot min^{-1}$ under stirring in an ice bath to neutralize the generated HCl. The gathered $Fe(acac)_3$ was further immersed in ultrapure water for 30 min in an ice bath to remove the generated NaCl, which was then washed and collected via the vacuum filtration system. This process was repeated three times to remove the impurities. The washed $Fe(acac)_3$ powder was finally dried at 80 °C under vacuum for 12 h.

The purity and yield of home-made $Fe(acac)_3$ were also determined by means of HPLC via the similar method to that of $Cu(acac)_2$. The profile of peak areas versus the concentrations of standard $Fe(acac)_3$ solutions was plotted, where a linear correlation with $R^2 = 0.996$ was obtained (**Figure S13**). To determine the purity of home-made $Fe(acac)_3$, a methanol solution of $Fe(acac)_3$ with a concentration of approximately 200 $mg \cdot L^{-1}$ was prepared. The $Fe(acac)_3$ solution was then analyzed by using the same method. According to the peak areas and standard curve, the actual concentration of the $Fe(acac)_3$ solution was obtained. In this work, the purity of home-made $Fe(acac)_3$ ($P_{Fe(acac)3}$) was determined based on the following equation:

$$P_{Fe(acac)3} = \frac{C_{Fe(acac)3,a}}{C_{Fe(acac)3}} \times 100\% = \frac{193.0\ mg \cdot L^{-1}}{200.0\ mg \cdot L^{-1}} \times 100\% = 96.5\%$$

where $C_{Fe(acac)3,a}$ and $C_{Fe(acac)3}$ represented the actual concentration of the $Fe(acac)_3$ solution detected via HPLC and the theoretical concentration of the $Fe(acac)_3$ solution, respectively. The ultimate yield of home-made $Fe(acac)_3$ ($Y_{Fe(acac)3}$) was calculated via the following equation:

$$Y_{Fe(acac)3} = \frac{m_{Fe(acac)3} \times P_{Fe(acac)3}}{m_{Fe(acac)3,t}} \times 100\% = \frac{47.69\ g \times 96.5\%}{50\ g} \times 100\% = 92.0\%$$

where $m_{Fe(acac)3}$ and $m_{Fe(acac)3,t}$ were the actual and target mass of produced $Fe(acac)_3$, respectively.

Besides, the soaking liquid and filtrates during the synthesis of $Fe(acac)_3$ were gathered to detect the amount of Hacac and Fe species in them via HPLC and ICP-AES, respectively. In this work, the volumes of filtrates and soaking liquid were 275 and 370 mL, respectively. The volume of Hacac and the mass of Fe species were determined as 2.17 mL and 12.82 mg in filtrates, respectively. For the soaking liquid, approximately 0.30 mL of Hacac and 62.53 mg of Fe species was detected in it. In this work, the utilization efficiency of Hacac for the synthesis of $Fe(acac)_3$ ($U_{Hacac,Fe}$) was calculated in terms of the following equation:

$$U_{Hacac,Fe} = \frac{m_{Fe(acac)3} \times P_{Fe(acac)3} \times V_{Hacac} \times 3}{M_{Fe(acac)3} \times v_{Hacac,Fe}} \times 100\% = \frac{47.69\ g \times 96.5\%}{353.17\ g} = 91.5\%$$

where $M_{Fe(acac)3}$ and $v_{Hacac,Fe}$ were the molar mass of $Fe(acac)_3$ and the volume of Hacac used in the synthesis of $Fe(acac)_3$, respectively.

3.2 Standard fabrication of Fe_2O_3 NCs and recovery of solvents. In a typical synthesis of Fe_2O_3 NCs, 120 mL of ODE and 30 mL of OA were mixed together in a four-neck flask and then heated to 260 ℃ under stirring in N_2 gas flow. Subsequently, 30 g of home-made $Fe(acac)_3$ was gradually added into the solution in about 20 min through the customized sample injector, after which the mixture was held at 260 ℃ for another 20 min before it was cooled to room temperature. The products were separated by adding 800 mL of ethanol antisolvent to the reaction solution, followed by centrifugation at 12000 rpm for 10 min. The gathered products were further calcinated at 500 ℃ for 1 h in a muffle furnace to remove the residual organic solvents. Moreover, Hacac, ODE, and ethanol were also recovered during the synthesis of Fe_2O_3 NCs.

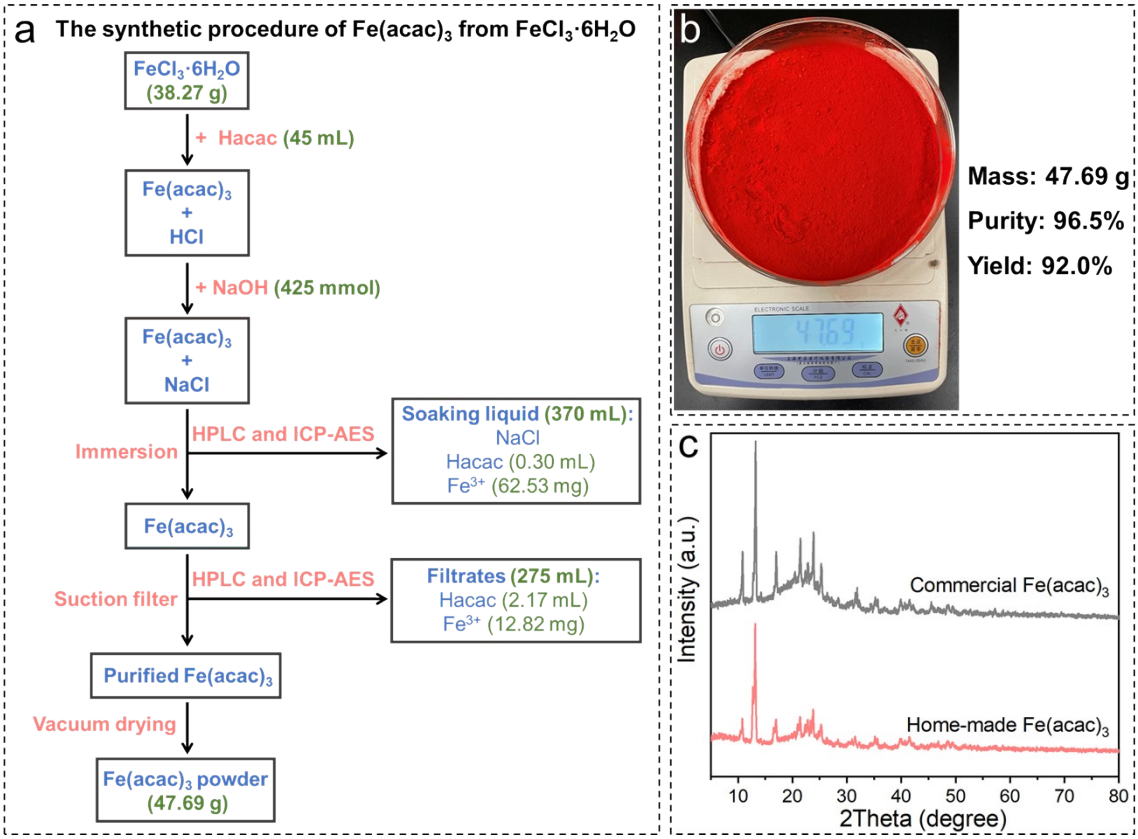

Figure S12. (a) The synthetic procedure of $Fe(acac)_3$ from $FeCl_3 \cdot 6H_2O$. (b) The picture of home-made $Fe(acac)_3$. (c) XRD profiles of home-made and commercial $Fe(acac)_3$.

In a single synthetic process of $Fe(acac)_3$ from $FeCl_3 \cdot 6H_2O$, 47.69 g of $Fe(acac)_3$ was produced with a purity of 96.5% and a yield of 92.0%. The utilization efficiency of Hacac was 91.5%. Only 2.17 mL of Hacac and 12.82 mg of Fe species were determined in filtrates.

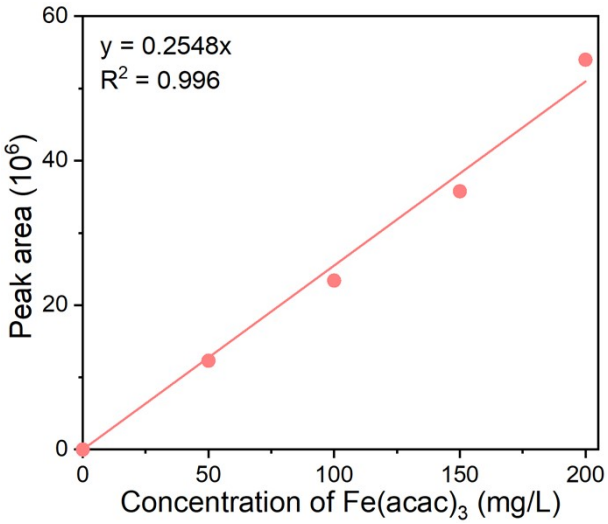

Figure S13. The standard curve of the detection of $Fe(acac)_3$ via HPLC.

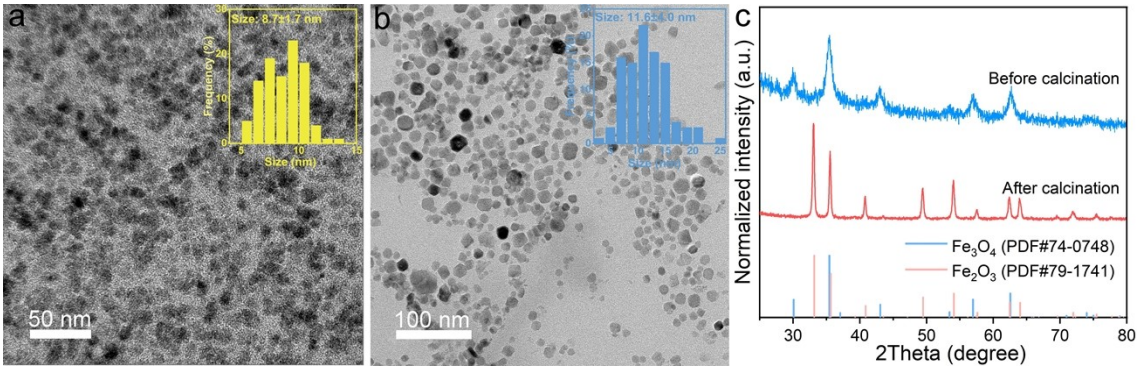

Figure S14. (a-b) TEM images and (c) XRD patterns of FeO_x before and after calcination. The insets in panels a and b were the size distribution histograms of Fe_3O_4 and Fe_2O_3 NCs, respectively.

4. Fabrication of Co_3O_4 NCs and recovery of organic ligands, synthesis, and purification solvents

4.1 Synthesis of $Co(acac)_2$ from $CoCl_2 \cdot 6H_2O$. In a typical synthesis of $Co(acac)_2$ with a target mass of 50 g, 46.26 g of $CoCl_2 \cdot 6H_2O$ was dissolved in 200 mL of ultrapure water in a 500-mL flask under magnetic stirring for 10 min to form a homogeneous solution. 41 mL of Hacac was then added into the flask under stirring in an ice bath for 30 min, during which Hacac chelated with Co^{2+} to form $Co(acac)_2$:

$$CoCl_2 \cdot 6H_2O + 2Hacac \rightarrow Co(acac)_2 + 2HCl + 6H_2O$$

100 mL of NaOH (3.89 M) was injected into the mixture at a rate of 3 $mL \cdot min^{-1}$ under stirring in an ice bath to neutralize the generated HCl. The gathered $Co(acac)_2$ was further immersed in ultrapure water for 30 min in an ice bath to remove the generated NaCl, which was then washed and collected via the vacuum filtration system. This process was repeated three times to remove the impurities. The washed $Co(acac)_2$ powder was finally dried at 80 °C under vacuum for 12 h.

The purity and yield of home-made $Co(acac)_2$ were also determined by means of HPLC. The profile of peak areas versus the concentrations of standard $Co(acac)_2$ solutions was plotted, where a linear correlation with $R^2 = 0.998$ was obtained (**Figure S16**). A methanol solution of $Co(acac)_2$ with a concentration of approximately 200 $mg \cdot L^{-1}$ was prepared to determine the purity of home-made $Co(acac)_2$. The $Co(acac)_2$ solution was then analyzed by using the same method. According to the peak areas and standard curve, the actual concentration of the $Co(acac)_2$ solution was obtained. In this work, the purity of home-made $Co(acac)_2$ ($P_{Co(acac)2}$) was determined via the following equation:

$$P_{Co(acac)2} = \frac{C_{Co(acac)2,a}}{C_{Co(acac)2}} \times 100\% = \frac{194.6\ mg \cdot L^{-1}}{200.0\ mg \cdot L^{-1}} \times 100\% = 97.3\%$$

where $C_{Co(acac)2,a}$ and $C_{Co(acac)2}$ represented the actual concentration of the $Co(acac)_2$ solution detected via HPLC and the theoretical concentration of the $Co(acac)_2$ solution, respectively. The ultimate yield of home-made $Co(acac)_2$ ($Y_{Co(acac)2}$) was calculated based on the following equation:

$$Y_{Co(acac)2} = \frac{m_{Co(acac)2} \times P_{Co(acac)2}}{m_{Co(acac)2,t}} \times 100\% = \frac{48.41\ g \times 97.3\%}{50\ g} \times 100\% = 94.2\%$$

where $m_{Co(acac)2}$ and $m_{Co(acac)2,t}$ were the actual and target mass of produced $Co(acac)_2$, respectively.

Besides, the soaking liquid and filtrates during the synthesis of $Co(acac)_2$ were gathered to detect the amount of Hacac and Co species in them via HPLC and ICP-AES, respectively. In this work, the volumes of filtrates and soaking liquid were 254 and 360 mL, respectively. The volume of Hacac and the mass of Co species were determined as 1.15 mL and 158.73 mg in filtrates, respectively. For the soaking liquid, approximately 0.04 mL of Hacac and 455.76 mg of Co species was detected in it. In this work, the utilization efficiency of Hacac for the synthesis of $Co(acac)_2$ ($U_{Hacac,Co}$) was calculated in terms of the following equation:

$$U_{Hacac,Co} = \frac{m_{Co(acac)2} \times P_{Co(acac)2} \times V_{Hacac} \times 2}{M_{Co(acac)2} \times v_{Hacac,Co}} \times 100\% = \frac{48.41\ g \times 97.3\%}{257.14\ g} = 94.1\%$$

where $M_{Co(acac)2}$ and $v_{Hacac,Co}$ were the molar mass of $Co(acac)_2$ and the volume of Hacac used in the synthesis of $Co(acac)_2$, respectively.

4.2 Standard fabrication of Co_3O_4 NCs and recovery of solvents. In a typical synthesis of Co_3O_4 NCs, 120 mL of ODE and 30 mL of OA were mixed together in a four-neck flask and then heated to 260 ℃ under stirring in N_2 gas flow. Subsequently, 30 g of home-made $Co(acac)_2$ was added into the solution within about 20 min through a customized sample injector, after which the mixture was held at 260 ℃ for another 20 min before it was cooled to room temperature. The products were separated by adding 800 mL of ethanol antisolvent to the reaction solution, followed by centrifugation at 12000 rpm for 10 min. The gathered products were further calcinated at 500 ℃ for 1 h in a muffle furnace to remove the residual organic solvents. Moreover, Hacac, ODE, and ethanol were also recovered during the synthesis of Co_3O_4 NCs.

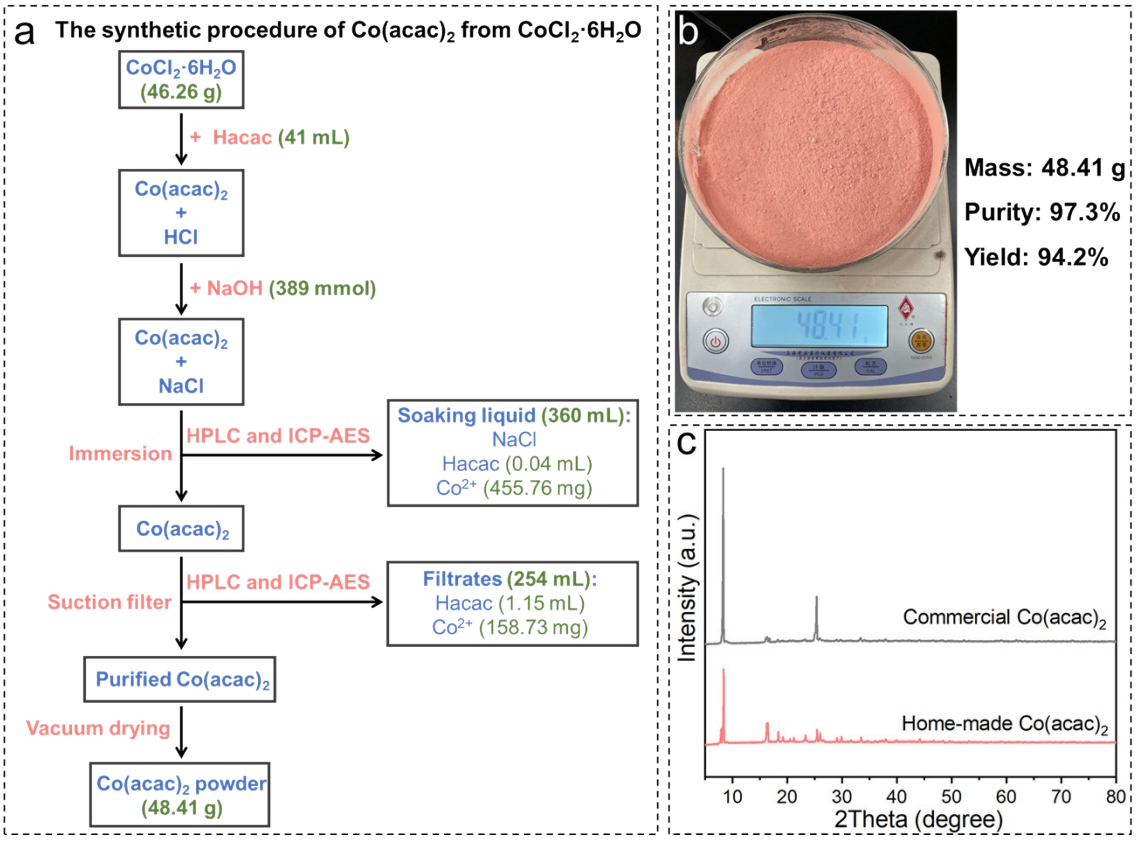

Figure S15. (a) The synthetic procedure of $Co(acac)_2$ from $CoCl_2 \cdot 6H_2O$. (b) The picture of home-made $Co(acac)_2$. (c) XRD profiles of home-made and commercial $Co(acac)_2$.

In a single synthetic process of $Co(acac)_2$ from $CoCl_2 \cdot 6H_2O$, 48.41 g of $Co(acac)_2$ was produced with a purity of 97.3% and a yield of 94.2%. The utilization efficiency of Hacac was 94.1%. Only 1.15 mL of Hacac and 158.73 mg of Co species were determined in filtrates.

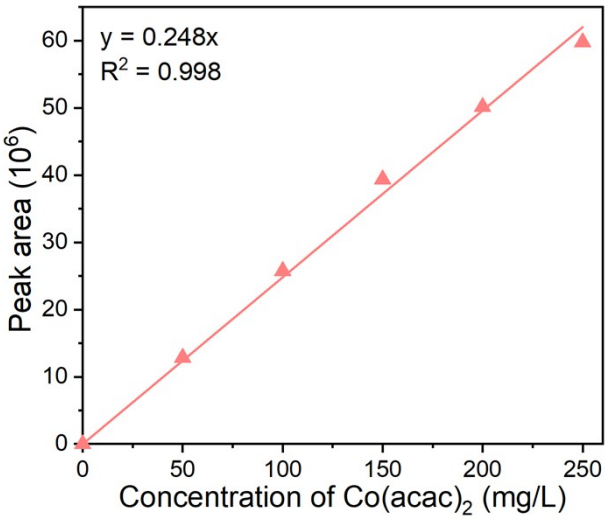

Figure S16. The standard curve of the detection of $Co(acac)_2$ via HPLC.

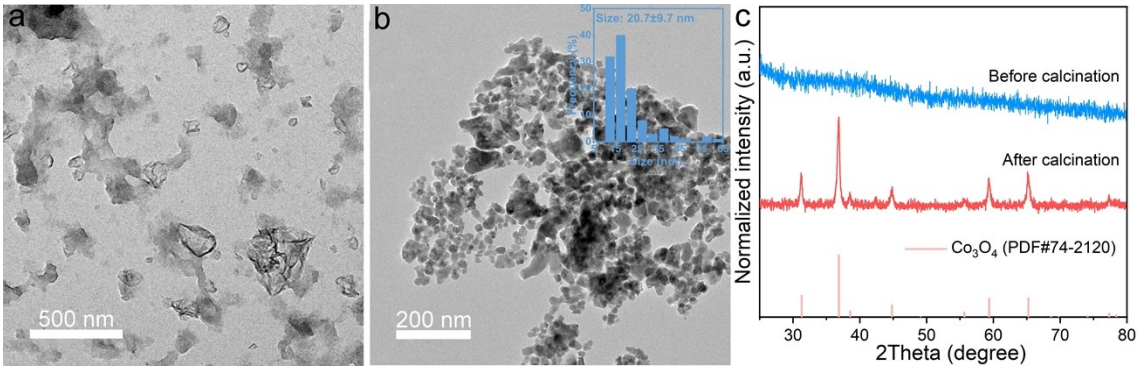

Figure S17. (a-b) TEM images and (c) XRD patterns of Co_3O_4 NCs before and after calcination. The inset in panel b was the size distribution histogram of Co_3O_4 NCs after calcination.

5. Fabrication of NiO_x NCs and recovery of organic ligands, synthesis, and purification solvents

5.1 Synthesis of $Ni(acac)_2$ from $NiCl_2·6H_2O$. In a typical synthesis of $Ni(acac)_2$ with a target mass of 50 g, 46.26 g of $NiCl_2·6H_2O$ was dissolved in 200 mL of ultrapure water in a 500-mL flask under magnetic stirring for 10 min to form a homogeneous solution. 41 mL of Hacac was then added into the flask under stirring in an ice bath for 30 min, during which Hacac chelated with Ni^{2+} to form $Ni(acac)_2$:

$$NiCl_2·6H_2O + 2Hacac \rightarrow Ni(acac)_2 + 2HCl + 6H_2O$$

100 mL of NaOH (3.89 M) was injected into the mixture at a rate of 3 $mL·min^{-1}$ under stirring in an ice bath to neutralize the generated HCl. The gathered $Ni(acac)_2$ was further immersed in ultrapure water for 30 min in an ice bath to remove the generated NaCl, which was then washed and collected via the vacuum filtration system. This process was repeated three times to remove the impurities. The washed $Ni(acac)_2$ powder was finally dried at 80 °C under vacuum for 12 h.

The purity and yield of home-made $Ni(acac)_2$ were also determined by means of HPLC. The profile of peak areas versus the concentrations of standard $Ni(acac)_2$ solutions was plotted, where a linear correlation with $R^2 = 0.996$ was obtained (**Figure S19**). A methanol solution of $Ni(acac)_2$ with a concentration of approximately 200 $mg·L^{-1}$ was prepared to determine the purity of home-made $Ni(acac)_2$. The $Ni(acac)_2$ solution was then analyzed by using the same method. According to the peak areas and standard curve, the actual concentration of the $Ni(acac)_2$ solution was obtained. In this work, the purity of home-made $Ni(acac)_2$ ($P_{Ni(acac)2}$) was determined via the following equation:

$$P_{Ni(acac)2} = \frac{C_{Ni(acac)2,a}}{C_{Ni(acac)2}} \times 100\% = \frac{199.2\ mg \cdot L^{-1}}{200.0\ mg \cdot L^{-1}} \times 100\% = 99.6\%$$

where $C_{Ni(acac)2}$ and $C_{Ni(acac)2}$ represented the actual concentration of the $Ni(acac)_2$ solution detected via HPLC and the theoretical concentration of the $Ni(acac)_2$ solution, respectively. The ultimate yield of home-made $Ni(acac)_2$ ($Y_{Ni(acac)2}$) was calculated based on the following equation:

$$Y_{Ni(acac)2} = \frac{m_{Ni(acac)2} \times P_{Ni(acac)2}}{m_{Ni(acac)2,t}} \times 100\% = \frac{49.35\ g \times 99.6\%}{50\ g} \times 100\% = 98.3\%$$

where $m_{Ni(acac)2}$ and $m_{Ni(acac)2,t}$ were the actual and target mass of produced $Ni(acac)_2$, respectively.

Besides, the soaking liquid and filtrates during the synthesis of $Ni(acac)_2$ were gathered to detect the amount of Hacac and Ni species in them via HPLC and ICP-AES, respectively. In this work, the volumes of filtrates and soaking liquid were 246 and 380 mL, respectively. The volume of Hacac and the mass of Ni species were determined as 0.92 mL and 347.72 mg in filtrates, respectively. For the soaking liquid, approximately 0.35 mL of Hacac and 698.82 mg of Ni species was detected in it. In this work, the utilization efficiency of Hacac for the synthesis of $Ni(acac)_2$ ($U_{Hacac,Ni}$) was calculated in terms of the following equation:

$$U_{Hacac,Ni} = \frac{m_{Ni(acac)2} \times P_{Ni(acac)2} \times V_{Hacac} \times 2}{M_{Ni(acac)2} \times v_{Hacac,Ni}} \times 100\% = \frac{49.35\ g \times 98.3\%}{256.91\ g} = 98.3\%$$

where $M_{Ni(acac)2}$ and $v_{Hacac,Ni}$ were the molar mass of $Ni(acac)_2$ and the volume of Hacac used in the synthesis of $Ni(acac)_2$, respectively.

5.2 Standard fabrication of NiO_x NCs and recovery of solvents. In a typical synthesis of NiO_x NCs, 120 mL of ODE and 30 mL of OA were mixed together in a four-neck flask and then heated to 300 ℃ under stirring in N_2 gas flow. Subsequently, 30 g of home-made $Ni(acac)_2$ was added into the solution within approximately 20 min, after which the mixture was held at 300 ℃ for another 10 min before it was cooled to room temperature. The products were separated by adding 800 mL of ethanol antisolvent to the reaction solution, followed by centrifugation at 12000 rpm for 10 min. The gathered products were further calcinated at 500 ℃ for 1 h in a muffle furnace to remove the residual organic solvents. Moreover, Hacac, ODE, and ethanol were also recovered during the synthesis of NiO_x NCs.

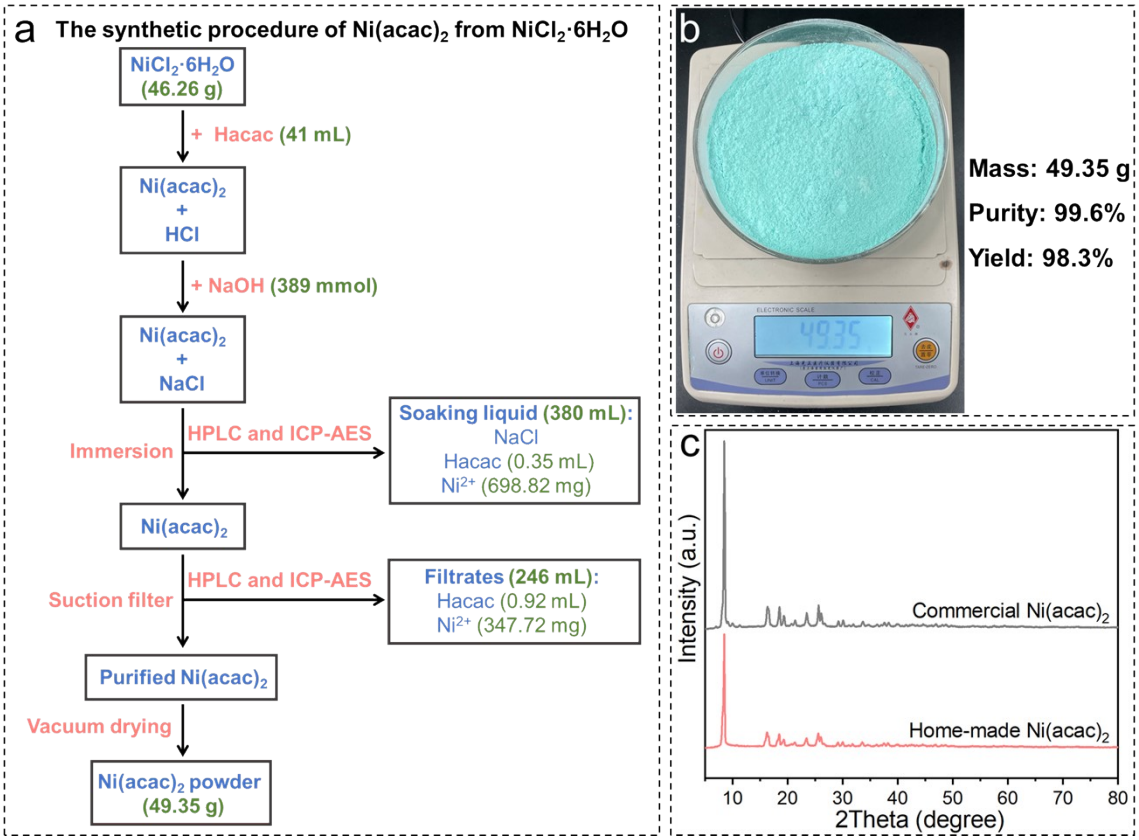

Figure S18. (a) The synthetic procedure of $Ni(acac)_2$ from $NiCl_2·6H_2O$. (b) The picture of home-made $Ni(acac)_2$. (c) XRD profiles of home-made and commercial $Ni(acac)_2$.

In a single synthetic process of $Ni(acac)_2$ from $NiCl_2·6H_2O$, 49.35 g of $Ni(acac)_2$ was produced with a purity of 99.6% and a yield of 98.3%. The utilization efficiency of Hacac was 98.3%. Only 0.92 mL of Hacac and 347.72 mg of Ni species were determined in filtrates.

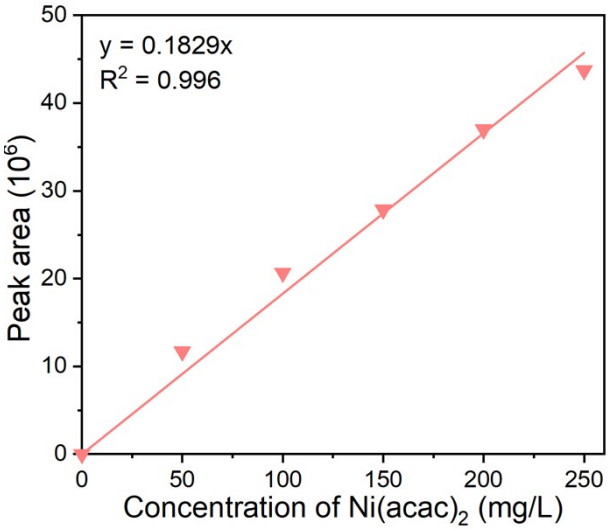

Figure S19. The standard curve of the detection of $Ni(acac)_2$ via HPLC.

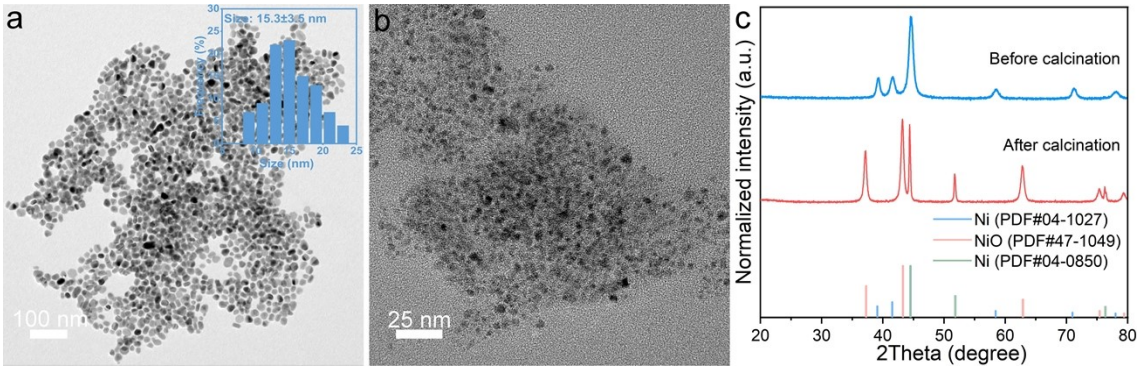

Figure S20. (a-b) TEM images and (c) XRD patterns of NiO_x NCs before and after calcination. The inset in panel a was the size distribution histogram of Ni NCs before calcination.

As shown in **Figure S20c**, hexagonal Ni NCs (PDF#04-1027) were directly obtained. The crystalline structure of NiO_x NCs after calcination was attributed to cubic Ni (PDF#04-0850) and NiO (PDF#47-1049) phases.

6. Fabrication of ZrO_2 NCs and recovery of organic ligands, synthesis, and purification solvents

6.1 Synthesis of $Zr(acac)_4$ from $ZrOCl_2 \cdot 8H_2O$. In a typical synthesis of $Zr(acac)_4$ with a target mass of 50 g, 33.04 g of $ZrOCl_2 \cdot 8H_2O$ was dissolved in 50 mL of ultrapure water in a 250-mL flask under magnetic stirring for 10 min to form a homogeneous solution. 43 mL of Hacac was then added into the flask under stirring in an ice bath for 30 min, during which Hacac chelated with Zr^{4+} to form $Zr(acac)_4$:

$$ZrOCl_2 \cdot 8H_2O + 4Hacac \rightarrow Zr(acac)_4 + 2HCl + 9H_2O$$

100 mL of NaOH (4.10 M) was injected into the mixture at a rate of 3 $mL \cdot min^{-1}$ under stirring in an ice bath to neutralize the generated HCl. The gathered $Zr(acac)_4$ was further immersed in ultrapure water for 30 min in an ice bath to remove the generated NaCl, which was then washed and collected via the vacuum filtration system. This process was repeated three times to remove the impurities. The washed $Zr(acac)_4$ powder was finally dried at 80 °C under vacuum for 12 h.

The purity and yield of home-made $Zr(acac)_4$ were also determined by means of HPLC. The profile of peak areas versus the concentrations of standard $Zr(acac)_4$ solutions was plotted, where a linear correlation with $R^2 = 0.999$ was obtained (**Figure S22**). A methanol solution of $Zr(acac)_4$ with a concentration of approximately 200 $mg \cdot L^{-1}$ was prepared to determine the purity of home-made $Zr(acac)_4$. The $Zr(acac)_4$ solution was then analyzed by using the same method. According to the peak areas and standard curve, the actual concentration of the $Zr(acac)_4$ solution was obtained. In this work, the purity of home-made $Zr(acac)_4$ ($P_{Zr(acac)4}$) was determined via the following equation:

$$P_{Zr(acac)4} = \frac{C_{Zr(acac)4,a}}{C_{Zr(acac)4}} \times 100\% = \frac{197.1\ mg \cdot L^{-1}}{200.0\ mg \cdot L^{-1}} \times 100\% = 98.5\%$$

where $C_{Zr(acac)4}$ and $C_{Zr(acac)4}$ represented the actual concentration of the $Zr(acac)_4$ solution detected via HPLC and the theoretical concentration of the $Zr(acac)_4$ solution, respectively. The ultimate yield of home-made $Zr(acac)_4$ ($Y_{Zr(acac)4}$) was calculated based on the following equation:

$$Y_{Zr(acac)4} = \frac{m_{Zr(acac)4} \times P_{Zr(acac)4}}{m_{Zr(acac)4,t}} \times 100\% = \frac{38.35\ g \times 98.5\%}{50\ g} \times 100\% = 75.6\%$$

where $m_{Zr(acac)4}$ and $m_{Zr(acac)4,t}$ were the actual and target mass of produced $Zr(acac)_4$, respectively.

Besides, the soaking liquid and filtrates during the synthesis of $Zr(acac)_4$ were gathered to detect the amount of Hacac and Zr species in them via HPLC and ICP-AES, respectively. In this work, the volumes of filtrates and soaking liquid were 120 and 254 mL, respectively. The volume of Hacac and the mass of Zr species were determined as 6.89 mL and 13.2 mg in filtrates, respectively. For the soaking liquid, approximately 0.60 mL of Hacac and 205.74 Zr species was detected in it. In this work, the utilization efficiency of Hacac for the synthesis of $Zr(acac)_4$ ($U_{Hacac,Zr}$) was calculated in terms of the following equation:

$$U_{Hacac,Zr} = \frac{m_{Zr(acac)4} \times P_{Zr(acac)4} \times V_{Hacac} \times 4}{M_{Zr(acac)4} \times v_{Hacac,Zr}} \times 100\% = \frac{38.35\ g \times 98.5\%}{491.69\ g} = 75.3\%$$

where $M_{Zr(acac)4}$ and $v_{Hacac,Zr}$ were the molar mass of $Zr(acac)_4$ and the volume of Hacac used in the synthesis of $Zr(acac)_4$, respectively.

6.2 Standard fabrication of ZrO_2 NCs and recovery of solvents. In a typical synthesis of ZrO_2 NCs, 150 mL of ODE was heated to 260 ℃ under stirring in N_2 gas flow in a four-neck flask. Subsequently, 30 g of home-made $Zr(acac)_4$ was added into the solution within approximately 20 min through a customized sample injector, after which the mixture was held at 260 ℃ for another 20 min before it was cooled to room temperature. The products were separated by direct centrifugation at 12000 rpm for 30 min, which were further calcinated at 500 ℃ for 1 h in a muffle furnace to remove the residual organic solvents. Moreover, Hacac, ODE, and ethanol were also recovered during the synthesis of ZrO_2 NCs.

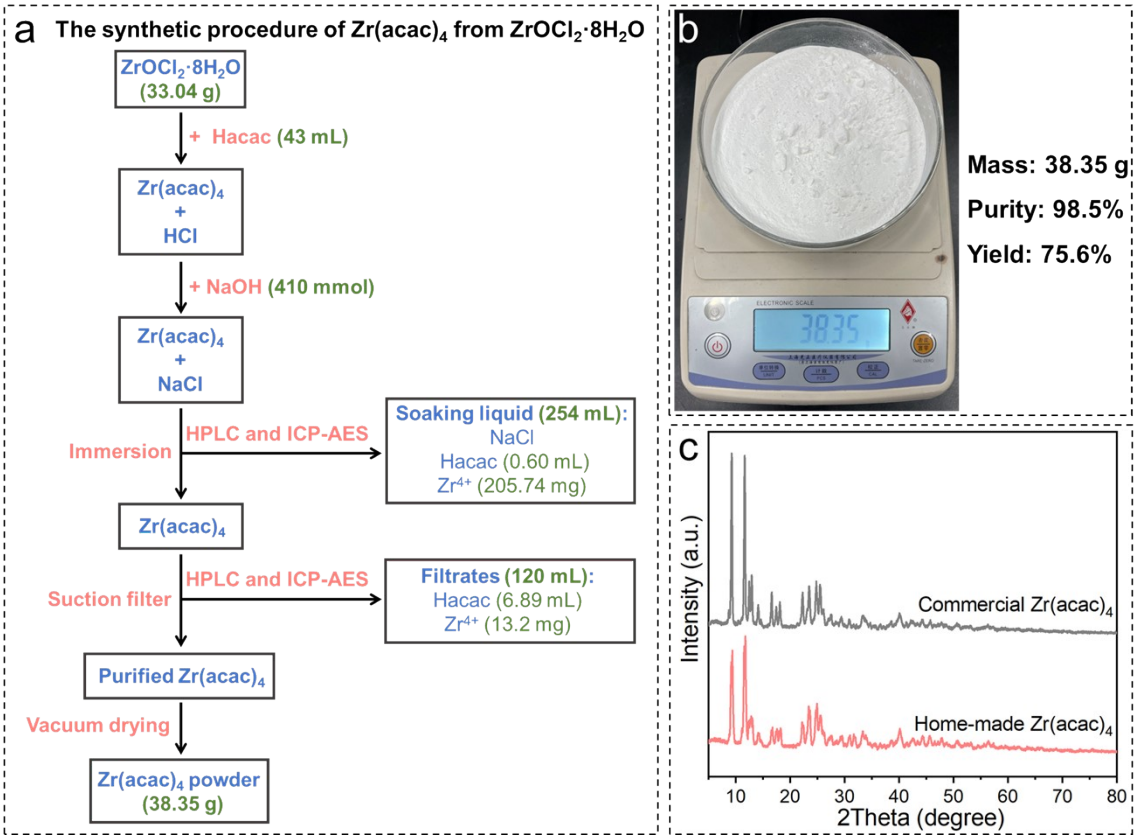

Figure S21. (a) The synthetic procedure of $Zr(acac)_4$ from $ZrOCl_2 \cdot 8H_2O$. (b) The picture of home-made $Zr(acac)_4$. (c) XRD profiles of home-made and commercial $Zr(acac)_4$.

In a single synthetic process of $Zr(acac)_4$ from $ZrOCl_2 \cdot 8H_2O$, 38.35 g of $Zr(acac)_4$ was produced with a purity of 98.5% and a yield of 75.6%. The utilization efficiency of Hacac was 75.3%. 6.89 mL of Hacac and 13.2 mg of Zr species were determined in filtrates.

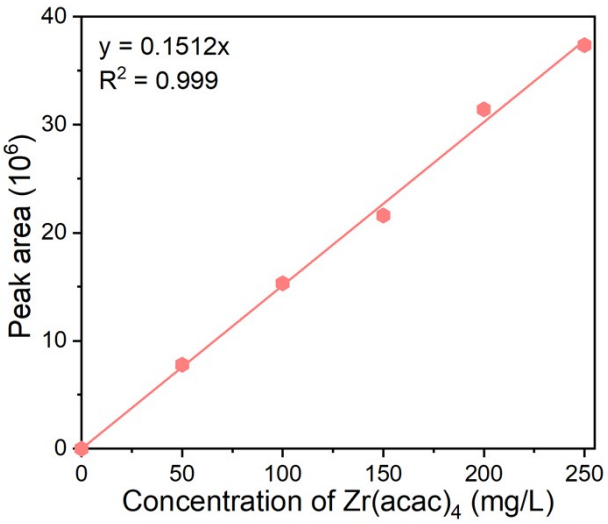

Figure S22. The standard curve of the detection of $Zr(acac)_4$ via HPLC.

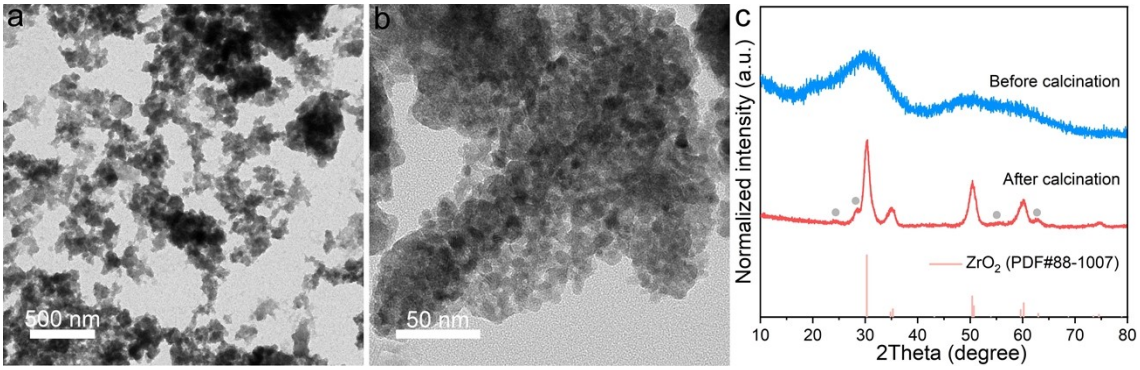

Figure S23. (a-b) TEM images and (c) XRD patterns of ZrO_2 NCs before and after calcination.

As shown in **Figure S23c**, ZrO_2 NCs after calcination were composed of tetragonal ZrO_2 phase (PDF#88-1007) and monoclinic ZrO_2 phase (marked with grey circles).

7. Fabrication of ZnO NCs and recovery of organic ligands, synthesis, and purification solvents

7.1 Synthesis of $Zn(acac)_2$ from $ZnCl_2$. In a typical synthesis of $Zn(acac)_2$ with a target mass of 50 g, 25.85 g of $ZnCl_2$ was dissolved in 200 mL of ultrapure water in a 500-mL flask under magnetic stirring for 10 min to form a homogeneous solution. 40 mL of Hacac was then added into the flask under stirring in an ice bath for 30 min, during which Hacac chelated with Zn^{2+} to form $Zn(acac)_2$:

$$ZnCl_2 + 2Hacac \rightarrow Zn(acac)_2 + 2HCl$$

100 mL of NaOH (3.79 M) was injected into the mixture at a rate of 3 $mL \cdot min^{-1}$ under stirring in an ice bath to neutralize the generated HCl. The gathered $Zn(acac)_2$ was further immersed in ultrapure water for 30 min in an ice bath to remove the generated NaCl, which was then washed and collected via the vacuum filtration system. This process was repeated three times to remove the impurities. The washed $Zn(acac)_2$ powder was finally dried at 40 °C under vacuum for 24 h.

The purity and yield of home-made $Zn(acac)_2$ were also determined by means of HPLC. The profile of peak areas versus the concentrations of standard $Zn(acac)_2$ solutions was plotted, where a linear correlation with $R^2 = 0.998$ was obtained (**Figure S25**). A methanol solution of $Zn(acac)_2$ with a concentration of approximately 200 $mg \cdot L^{-1}$ was prepared to determine the purity of home-made $Zn(acac)_2$. The $Zn(acac)_2$ solution was then analyzed by using the same method. According to the peak areas and standard curve, the actual concentration of the $Zn(acac)_2$ solution was obtained. In this work, the purity of home-made $Zn(acac)_2$ ($P_{Zn(acac)2}$) was determined via the following equation:

$$P_{Zn(acac)2} = \frac{C_{Zn(acac)2,a}}{C_{Zn(acac)2}} \times 100\% = \frac{196.5\ mg \cdot L^{-1}}{200.0\ mg \cdot L^{-1}} \times 100\% = 98.3\%$$

where $C_{Zn(acac)2}$ and $C_{Zn(acac)2}$ represented the actual concentration of the $Zn(acac)_2$ solution detected via HPLC and the theoretical concentration of the $Zn(acac)_2$ solution, respectively. The ultimate yield of home-made $Zn(acac)_2$ ($Y_{Zn(acac)2}$) was calculated based on the following equation:

$$Y_{Zn(acac)2} = \frac{m_{Zn(acac)2} \times P_{Zn(acac)2}}{m_{Zn(acac)2,t}} \times 100\% = \frac{45.23\ g \times 98.3\%}{50\ g} \times 100\% = 88.9\%$$

where $m_{Zn(acac)2}$ and $m_{Zn(acac)2,t}$ were the actual and target mass of produced $Zn(acac)_2$, respectively.

Besides, the soaking liquid and filtrates during the synthesis of $Zn(acac)_2$ were gathered to detect the amount of Hacac and Zn species in them via HPLC and ICP-AES, respectively. In this work, the volumes of filtrates and soaking liquid were 240 and 232 mL, respectively. The volume of Hacac and the mass of Zn species were determined as 0.91 mL and 385.20 mg in filtrates, respectively. For the soaking liquid, approximately 1.03 mL of Hacac and 590.44 mg of Zn species was detected in it. In this work, the utilization efficiency of Hacac for the synthesis of $Zn(acac)_2$ ($U_{Hacac,Zn}$) was calculated in terms of the following equation:

$$U_{Hacac,Zn} = \frac{m_{Zn(acac)2} \times P_{Zn(acac)2} \times V_{Hacac} \times 2}{M_{Zn(acac)2} \times v_{Hacac,Zn}} \times 100\% = \frac{45.23\ g \times 98.3\%}{263.6\ g \cdot} = 88.7\%$$

where $M_{Zn(acac)2}$ and $v_{Hacac,Zn}$ were the molar mass of $Zn(acac)_2$ and the volume of Hacac used in the synthesis of $Zn(acac)_2$, respectively.

7.2 Standard fabrication of ZnO NCs and recovery of solvents. In a typical synthesis of ZnO NCs, 150 mL of ODE were heated to 260 ℃ under stirring in N_2 gas flow in a four-neck flask. Subsequently, 30 g of home-made $Zn(acac)_2$ was added into the solution within approximately 20 min through a customized sample injector, after which the mixture was held at 250 ℃ for another 20 min before it was cooled to room temperature. ZnO NCs as products were separated by direct centrifugation at 12000 rpm for 30 min, which were further calcinated at 400 ℃ for 1 h in a muffle furnace to remove the residual organic solvents. Moreover, Hacac, ODE, and ethanol were also recovered during the synthesis of ZnO NCs.

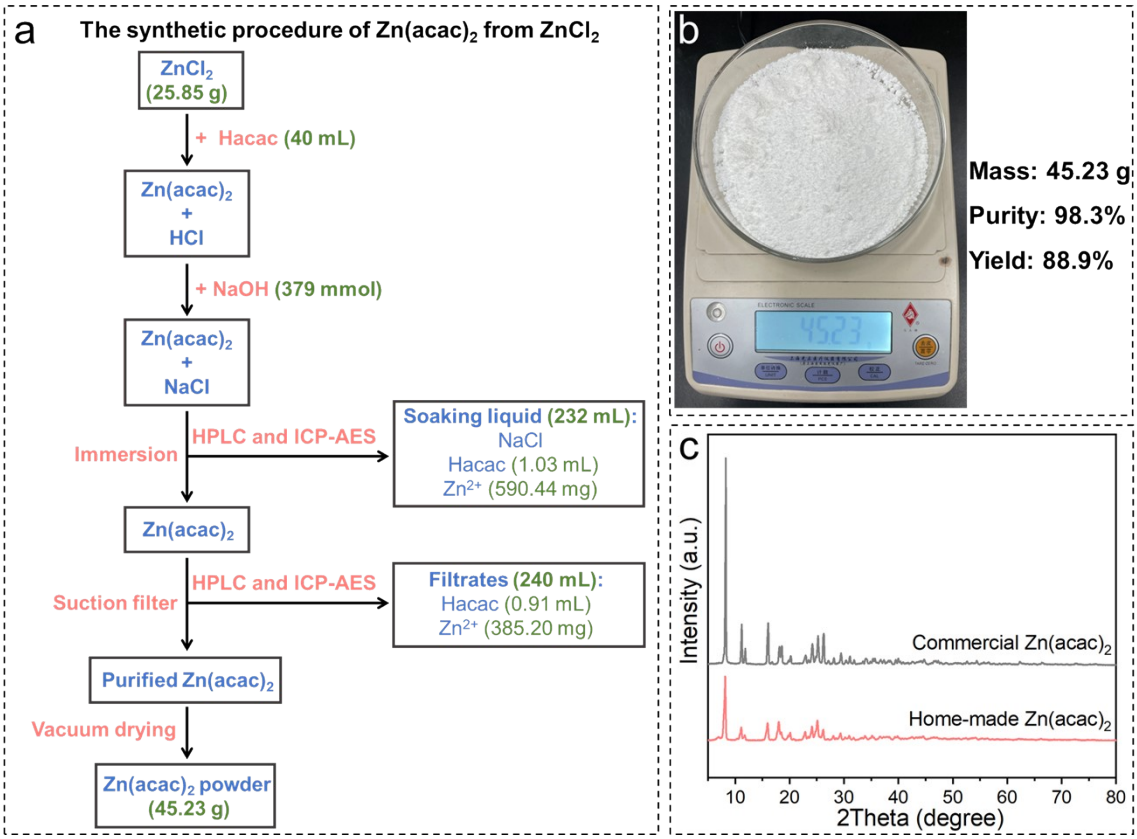

Figure S24. (a) The synthetic procedure of $Zn(acac)_2$ from $ZnCl_2$. (b) The picture of home-made $Zn(acac)_2$. (c) XRD profiles of home-made and commercial $Zn(acac)_2$.

In a single synthetic process of $Zn(acac)_2$ from $ZnCl_2$, 45.23 g of $Zn(acac)_2$ was produced with a purity of 98.3% and a yield of 88.9%. The utilization efficiency of Hacac was 88.7%. Only 0.91 mL of Hacac and 385.20 mg of Zn species were determined in filtrates.

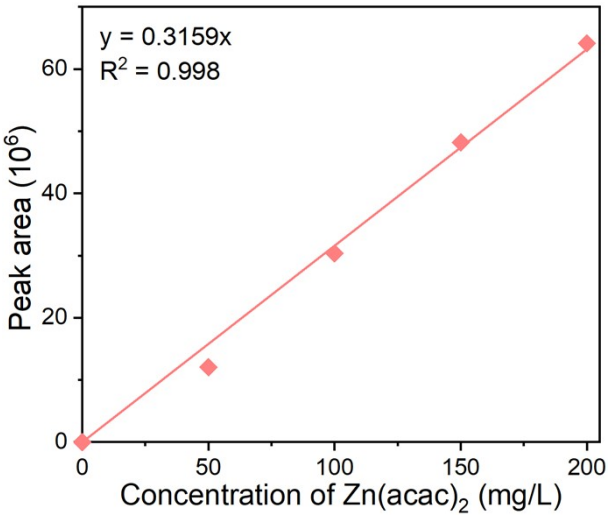

Figure S25. The standard curve of the detection of $Zn(acac)_2$ via HPLC.

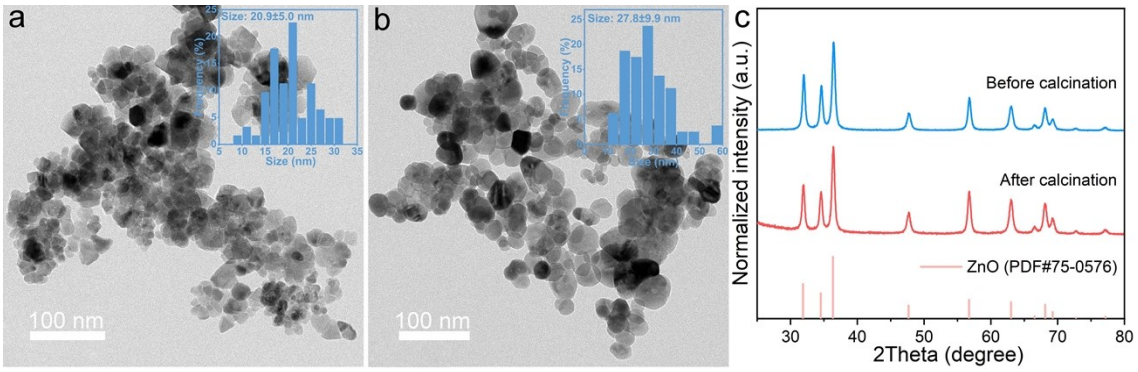

Figure S26. TEM images of ZnO NCs (a) before and (b) after calcination. The insets in panels a and b were the size distribution histograms of ZnO NCs before and after calcination. (c) XRD patterns of ZnO NCs before and after calcination.

8. Fabrication of CeO_2 NCs and recovery of organic ligands, synthesis, and purification solvents

8.1 Synthesis of $Ce(acac)_3$ from $CeCl_3 \cdot 7H_2O$. In a typical synthesis of $Ce(acac)_3$ with a target mass of 50 g, 42.59 g of $CeCl_3 \cdot 7H_2O$ was dissolved in 200 mL of ultrapure water in a 500-mL flask under magnetic stirring for 10 min to form a homogeneous solution. 36 mL of Hacac was then added into the flask under stirring in an ice bath for 30 min, during which Hacac chelated with Ce^{3+} to form $Ce(acac)_3$:

$$CeCl_3 \cdot 7H_2O + 3Hacac \rightarrow Ce(acac)_3 + 3HCl + 7H_2O$$

100 mL of NaOH (3.43 M) was injected into the mixture at a rate of 3 $mL \cdot min^{-1}$ under stirring in an ice bath to neutralize the generated HCl. The gathered $Ce(acac)_3$ was further immersed in ultrapure water for 30 min in an ice bath to remove the generated NaCl, which was then washed and collected via the vacuum filtration system. This process was repeated three times to remove the impurities. The washed $Ce(acac)_3$ powder was finally dried at 80 °C under vacuum for 12 h.

The purity and yield of home-made $Ce(acac)_3$ were also determined by means of HPLC. The profile of peak areas versus the concentrations of standard $Ce(acac)_3$ solutions was plotted, where a linear correlation with $R^2 = 0.996$ was obtained (**Figure S28**). A methanol solution of $Ce(acac)_3$ with a concentration of approximately 200 $mg \cdot L^{-1}$ was prepared to determine the purity of home-made $Ce(acac)_3$. The $Ce(acac)_3$ solution was then analyzed by using the same method. According to the peak areas and standard curve, the actual concentration of the $Ce(acac)_3$ solution was obtained. In this work, the purity of home-made $Ce(acac)_3$ ($P_{Ce(acac)3}$) was determined via the following equation:

$$P_{Ce(acac)3} = \frac{C_{Ce(acac)3,a}}{C_{Ce(acac)3}} \times 100\% = \frac{183.1\ mg \cdot L^{-1}}{200.0\ mg \cdot L^{-1}} \times 100\% = 91.6\%$$

where $C_{Ce(acac)3,a}$ and $C_{Ce(acac)3}$ represented the actual concentration of the $Ce(acac)_3$ solution detected via HPLC and the theoretical concentration of the $Ce(acac)_3$ solution, respectively. The ultimate yield of home-made $Ce(acac)_3$ ($Y_{Ce(acac)3}$) was calculated based on the following equation:

$$Y_{Ce(acac)3} = \frac{m_{Ce(acac)3} \times P_{Ce(acac)3}}{m_{Ce(acac)3,t}} \times 100\% = \frac{47.98\ g \times 91.6\%}{50\ g} \times 100\% = 87.8\%$$

where $m_{Ce(acac)3}$ and $m_{Ce(acac)3,t}$ were the actual and target mass of produced $Ce(acac)_3$, respectively.

Besides, the soaking liquid and filtrates during the synthesis of $Ce(acac)_3$ were gathered to detect the amount of Hacac and Ce species in them via HPLC and ICP-AES, respectively. In this work, the volumes of filtrates and soaking liquid were 240 and 362 mL, respectively. The volume of Hacac and the mass of Ce species were determined as 0.03 mL and 12.00 mg in filtrates, respectively. For the soaking liquid, approximately 0.03 mL of Hacac and 17.01 mg of Ce species was detected in it. In this work, the utilization efficiency of Hacac for the synthesis of $Ce(acac)_3$ ($U_{Hacac,Ce}$) was calculated in terms of the following equation:

$$U_{Hacac,Ce} = \frac{m_{Ce(acac)3} \times P_{Ce(acac)3} \times V_{Hacac} \times 3}{M_{Ce(acac)3} \times v_{Hacac,Ce}} \times 100\% = \frac{47.98\ g \times 91.6\%}{437.44\ g} = 88.1\%$$

where $M_{Ce(acac)3}$ and $v_{Hacac,Ce}$ were the molar mass of $Ce(acac)_3$ and the volume of Hacac used in the synthesis of $Ce(acac)_3$, respectively.

8.2 Standard fabrication of CeO_2 NCs and recovery of solvents. In a typical synthesis of CeO_2 NCs, 120 mL of ODE, 18 mL of OAm, and 12 mL of OA were mixed together in a four-neck flask and then heated to 260 ℃ under stirring in N_2 gas flow. The mixture was maintained at 260 ℃ for 10 min to form a stable transparent solution. Subsequently, 30 g of home-made $Ce(acac)_3$ was added into the solution over approximately 20 min through a customized sample injector, after which the mixture was held at 260 ℃ for another 20 min before it was cooled to room temperature. The products were separated by direct centrifugation at 12000 rpm for 20 min, which were further calcinated at 400 ℃ for 1 h in a muffle furnace to remove the residual organic solvents. Moreover, Hacac, ODE, and ethanol were also recovered during the synthesis of CeO_2 NCs.

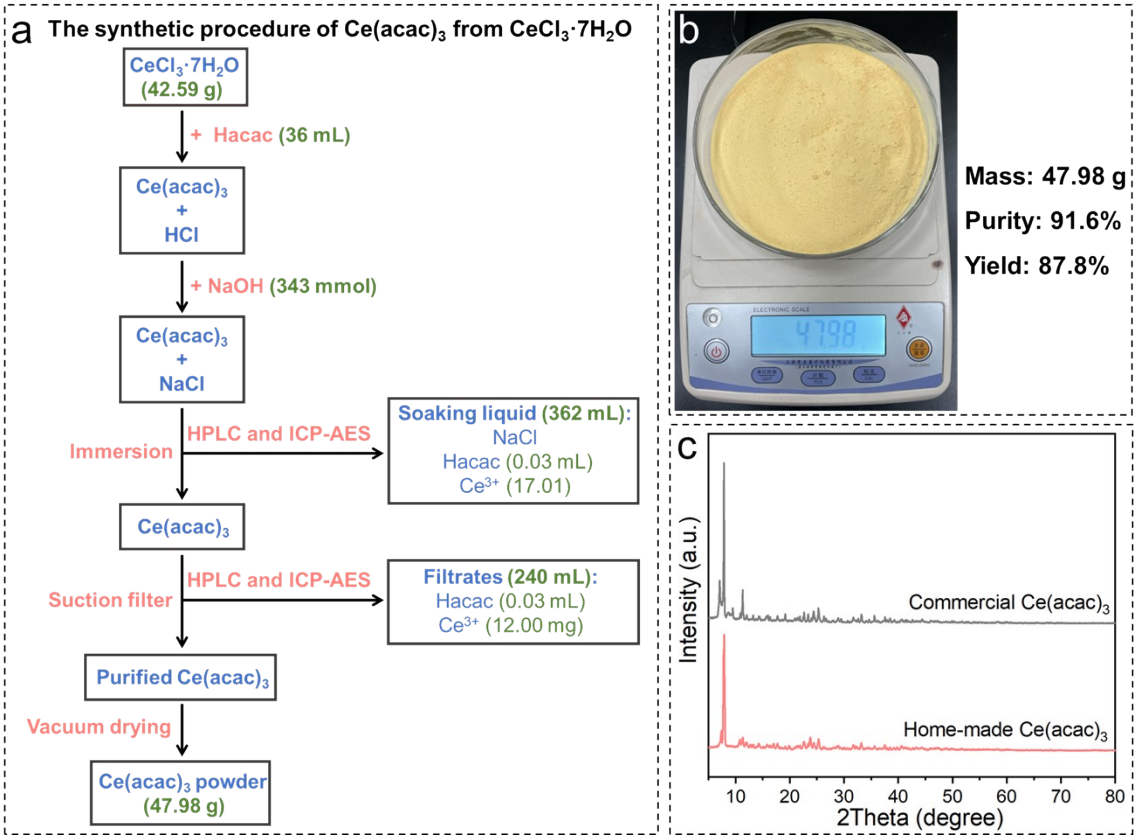

Figure S27. (a) The synthetic procedure of $Ce(acac)_3$ from $CeCl_3 \cdot 7H_2O$. (b) The picture of home-made $Ce(acac)_3$. (c) XRD profiles of home-made and commercial $Ce(acac)_3$.

In a single synthetic process of $Ce(acac)_3$ from $CeCl_3$, 47.98 g of $Ce(acac)_3$ was produced with a purity of 91.6% and a yield of 87.8%. The utilization efficiency of Hacac was 88.1%. Only 0.03 mL of Hacac and 12.00 mg of Ce species were determined in filtrate.

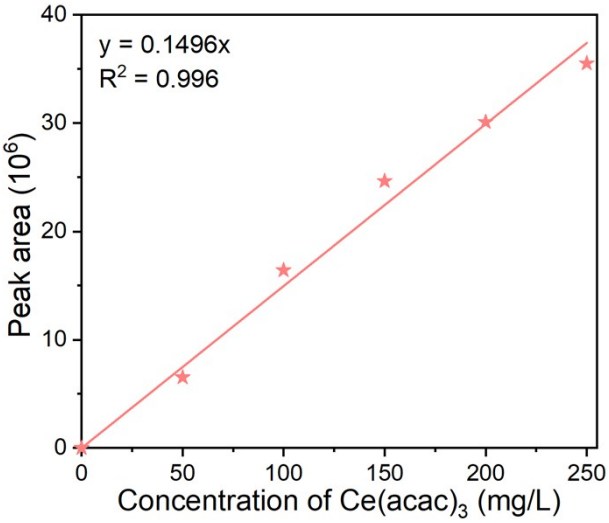

Figure S28. The standard curve of the detection of $Ce(acac)_3$ via HPLC.

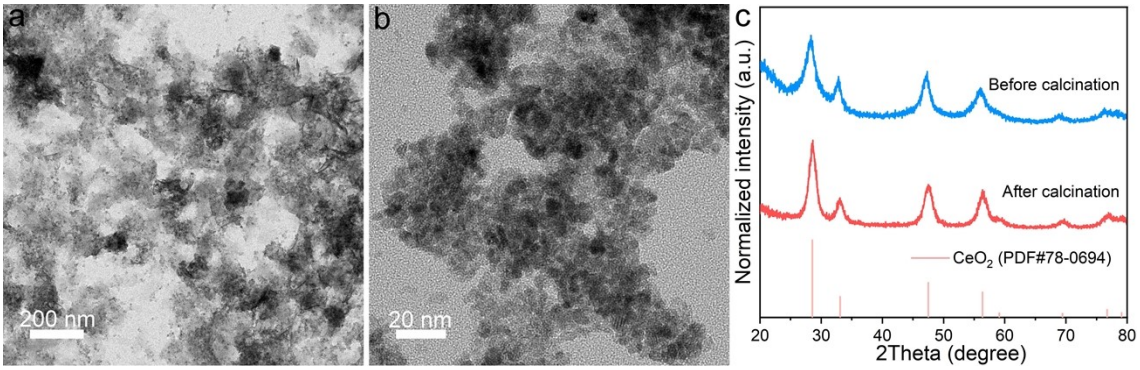

Figure S29. TEM images of CeO_2 NCs (a) before and (b) after calcination. (c) XRD patterns of CeO_2 NCs before and after calcination.

9. Fabrication of Mn_3O_4 NCs and recovery of organic ligands, synthesis and purification solvents

9.1 Synthesis of $Mn(acac)_2$ from $MnSO_4 \cdot H_2O$. In a typical synthesis of $Mn(acac)_2$ with a target mass of 50 g, 33.38 g of $MnSO_4 \cdot H_2O$ was dissolved in 200 mL of ultrapure water in a 500-mL flask under magnetic stirring for 10 min to form a homogeneous solution. 42 mL of Hacac was then added into the flask under stirring in an ice bath for 30 min, during which Hacac chelated with Mn^{2+} to form $Mn(acac)_2$:

$$MnSO_4 \cdot H_2O + 2Hacac \rightarrow Mn(acac)_2 + H_2SO_4 + H_2O$$

100 mL of NaOH (3.95 M) was injected into the mixture at a rate of 3 $mL \cdot min^{-1}$ under stirring in an ice bath to neutralize the generated H_2SO_4. The gathered $Mn(acac)_2$ was further immersed in ultrapure water for 30 min in an ice bath to remove the generated $NaSO_4$, which was then washed and collected via the vacuum filtration system. This process was repeated three times to remove the impurities. The washed $Mn(acac)_2$ powder was finally dried at 80 °C under vacuum for 12 h.

The purity and yield of home-made $Mn(acac)_2$ were also determined by means of HPLC. The profile of peak areas versus the concentrations of standard $Mn(acac)_2$ solutions was plotted, where a linear correlation with $R^2 = 0.998$ was obtained (**Figure S31**). A methanol solution of $Mn(acac)_2$ with a concentration of approximately 200 $mg \cdot L^{-1}$ was prepared to determine the purity of home-made $Mn(acac)_2$. The $Mn(acac)_2$ solution was then analyzed by using the same method. According to the peak areas and standard curve, the actual concentration of the $Mn(acac)_2$ solution was obtained. In this work, the purity of home-made $Mn(acac)_2$ ($P_{Mn(acac)2}$) was determined via the following equation:

$$P_{Mn(acac)2} = \frac{C_{Mn(acac)2,a}}{C_{Mn(acac)2}} \times 100\% = \frac{197.1\ mg \cdot L^{-1}}{200.0\ mg \cdot L^{-1}} \times 100\% = 98.5\%$$

where $C_{Mn(acac)2,a}$ and $C_{Mn(acac)2}$ represented the actual concentration of the $Mn(acac)_2$ solution detected via HPLC and the theoretical concentration of the $Mn(acac)_2$ solution, respectively. The ultimate yield of home-made $Mn(acac)_2$ ($Y_{Mn(acac)2}$) was calculated based on the following equation:

$$Y_{Mn(acac)2} = \frac{m_{Mn(acac)2} \times P_{Mn(acac)2}}{m_{Mn(acac)2,t}} \times 100\% = \frac{42.90\ g\ \times\ 98.5\%}{50\ g} \times 100\% = 84.6\%$$

where $m_{Mn(acac)2}$ and $m_{Mn(acac)2,t}$ were the actual and target mass of produced $Mn(acac)_2$, respectively.

Besides, the soaking liquid and filtrates during the synthesis of $Mn(acac)_2$ were gathered to detect the amount of Hacac and Mn species in them via HPLC and ICP-AES, respectively. In this work, the volumes of filtrates and soaking liquid were 200 and 260 mL, respectively. The volume of Hacac and the mass of Mn species were determined as 0.03 mL and 247.00 mg in filtrates, respectively. For the soaking liquid, approximately 0.43 mL of Hacac and 513.50 mg of Mn species was detected in it. In this work, the utilization efficiency of Hacac for the synthesis of $Mn(acac)_2$ ($U_{Hacac,Mn}$) was calculated in terms of the following equation:

$$U_{Hacac,Mn} = \frac{m_{Mn(acac)2} \times P_{Mn(acac)2} \times V_{Hacac} \times 2}{M_{Mn(acac)2} \times v_{Hacac,Mn}} \times 100\% = \frac{42.90\ g\ \times\ 98.5\%\ \times}{253.15\ g \cdot r} = 83.7\%$$

where $M_{Mn(acac)2}$ and $v_{Hacac,Mn}$ were the molar mass of $Mn(acac)_2$ and the volume of Hacac used in the synthesis of $Mn(acac)_2$, respectively.

9.2 Standard fabrication of Mn_3O_4 NCs and recovery of synthesis solvents. In a typical synthesis of Mn_3O_4 NCs, 120 mL of ODE and 30 mL of OA were mixed together in a four-neck flask and then heated to 260 ℃ under stirring in N_2 gas flow. Subsequently, 30 g of home-made $Mn(acac)_2$ was added into the solution within around 20 min through a customized sample injector, after which the mixture was held at 260 ℃ for another 20 min before it was cooled to room temperature. Mn_3O_4 NCs as products were separated by adding 800 mL of ethanol antisolvent to the reaction solution, followed by centrifugation at 12000 rpm for 10 min. Mn_3O_4 NCs were further calcinated at 400 ℃ for 1 h in a muffle furnace to remove the residual organic solvents. Moreover, Hacac, ODE, and ethanol were also recovered during the synthesis of Mn_3O_4 NCs.

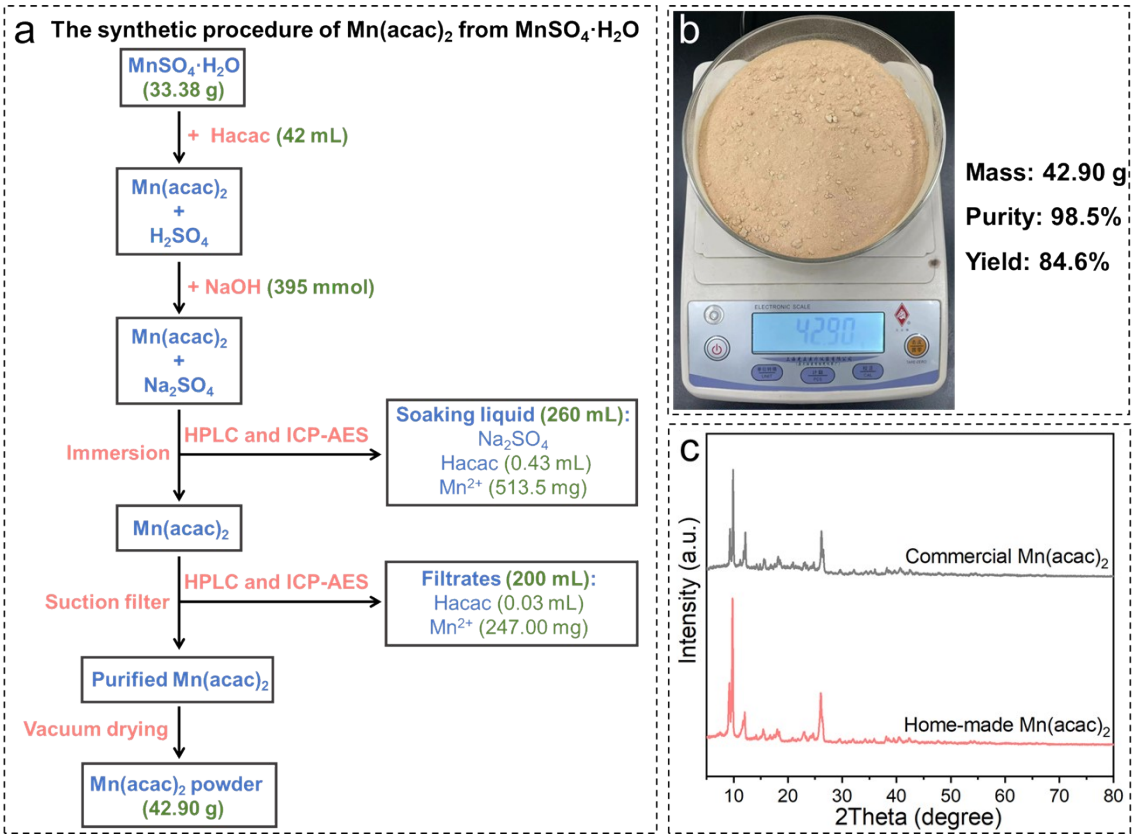

Figure S30. (a) The synthetic procedure of $Mn(acac)_2$ from $MnSO_4 \cdot H_2O$. (b) The picture of home-made $Mn(acac)_2$. (c) XRD profiles of home-made and commercial $Mn(acac)_2$.

In a single synthetic process of $Mn(acac)_2$ from $MnSO_4 \cdot H_2O$, 42.90 g of $Mn(acac)_2$ was produced with a purity of 98.5% and a yield of 84.6%. The utilization efficiency of Hacac was 83.7%. Only 0.03 mL of Hacac and 237.00 mg of Mn species were determined in filtrates.

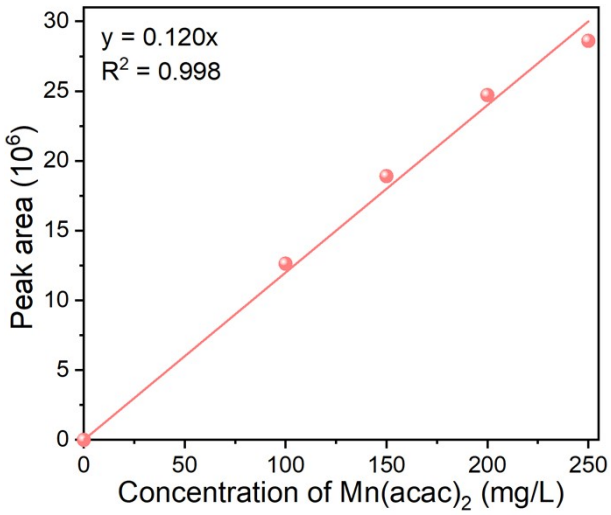

Figure S31. The standard curve of the detection of $Mn(acac)_2$ via HPLC.

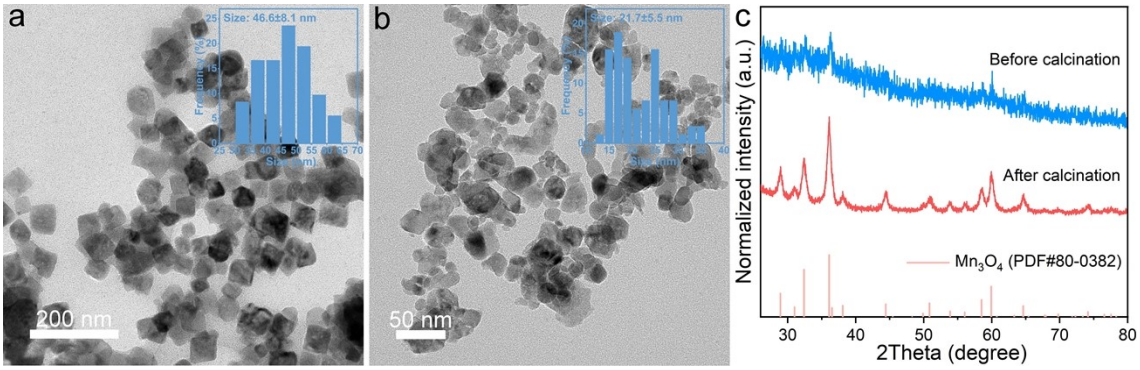

Figure S32. TEM images of Mn_3O_4 NCs (a) before and (b) after calcination. The insets in panels a and b were the size distribution histograms of Mn_3O_4 NCs before and after calcination, respectively. (c) XRD patterns of Mn_3O_4 NCs before and after calcination.

Table S1. The amount of chemicals used during the synthesis of $M(acac)_x$ with a target mass of 50 g.

$M(acac)_x$	Metal precursor (g)	Hacac (mL)	100 mL of NaOH (M)
$Cu(acac)_2$	47.75 g, $CuSO_4 \cdot 5H_2O$	41	3.82
$Fe(acac)_3$	38.27 g, $FeCl_3 \cdot 6H_2O$	45	4.25
$Co(acac)_2$	46.26 g, $CoCl_2 \cdot 6H_2O$	41	3.89
$Ni(acac)_2$	46.26 g, $NiCl_2 \cdot 6H_2O$	41	3.89
$Zr(acac)_4$	33.04 g, $ZrOCl_2 \cdot 8H_2O$	43	4.10
$Zn(acac)_2$	25.85 g, $ZnCl_2$	40	3.79
$Ce(acac)_3$	42.59 g, $CeCl_3 \cdot 7H_2O$	36	3.43
$Mn(acac)_2$	33.38 g, $MnSO_4 \cdot H_2O$	42	3.95

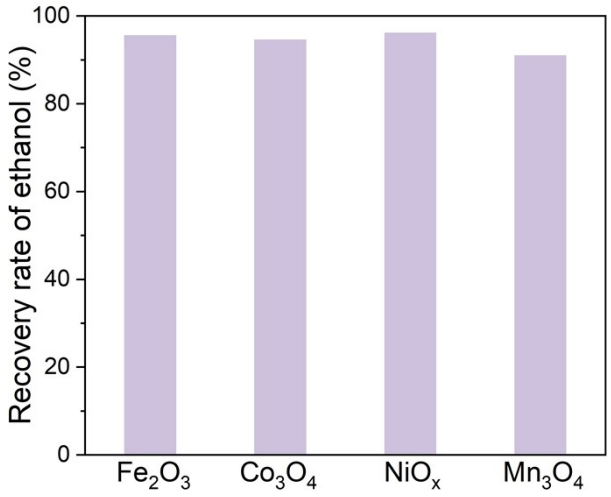

Figure S33. Recovery rates of ethanol during the synthesis of MO_x NCs.

It's worth mentioning that ethanol was not utilized during the synthesis of ZrO_2, ZnO, and CeO_2 NCs.

Table S2. Summary of fabrication of metal or MO_x NCs using traditional colloidal synthesis methods.

NCs	Precursor	M_{pre} (g)[a]	Solvent	V_{sol} (mL)[b]	Surfactant	V_{sur} (mL)[c]	T (°C)	Yield (g)	Ref.
CuO	$Cu(acac)_2$	30	ODE	120	OA	30	260	9.12	*This work*
Fe_3O_4	Fe-OA	36	ODE	254	OA	6.4	300	40	S4
Fe_3O_4	$Fe(acac)_3$	100	hexadecanol	490	/	/	300	20.3	S5
Fe_3O_4	$Fe(acac)_3$	22	ODE	400	OA/OAm	19/65	230	6	S6
MnO_x	$Mn(acac)_2$	5.1	OAm	123	dihydroxynaphthalene	6	300	3.8	S7
ZnO	Zn-OA	18	OAm	300	OA	90	300	2.83	S8
ZrO_2	$Zr(OC_3H_7)_4 \cdot C_3H_7OH$	66.6	benzyl alcoho	600	/	/	210	/	S9
CeO_2	$CeCl_3$	15.6	OAm	200	/	/	265	/	S10
CeO_2	$Ce(NO_3)_3$	17	OAm	200	OA	38	320	10	S11

[a] M_{pre}, the mass of metal precursors. [b] V_{sol}, the volume of synthesis solvents. [c] V_{sur}, the volume of surfactants.

Table S3. Brunauer-Emmett-Teller (BET) surface areas of as-obtained MO_x NCs.

Sample	BET surface area (m^2/g)
CuO	34.5
Fe_2O_3	37.3
Co_3O_4	33.1
NiO_x	54.6
ZrO_2	54.3
ZnO	31.2
CeO_2	131.8
Mn_3O_4	25.7

10. Multi-round fabrication of multimetallic oxide NCs with recovered solvents

10.1 Standard fabrication of $CuO/ZnO/ZrO_2$ NCs. The fabrication of multimetallic oxide NCs and recovery of solvents were also via the solid hot-injection solvent-recycle method in this work. Take the synthesis of $CuO/ZnO/ZrO_2$ NCs with a CuO molar ratio of 4.5% (named as 4.5%-$CuO/ZnO/ZrO_2$) as an example. 140 mL of ODE and 10 mL of OA were mixed together in a four-neck flask and then heated to 260 ℃ under stirring in N_2 gas flow. 2.19 g of $Zn(acac)_2$ and 27.05 g of $Zr(acac)_4$ were homogeneously mixed together and then added into the solution within around 20 min through the customized sample injector, which was held at 260 ℃ for another 20 min. After cooled down to room temperature, 0.79 g of $Cu(acac)_2$ was subsequently added into the ZnO/ZrO_2-containing solution. The mixture was kept at 120 ℃ for 10 min and then heated to 260 ℃ for 10 min. The products were separated by adding 800 mL of ethanol antisolvent to the reaction solution, followed by centrifugation at 12000 rpm for 20 min. The gathered products were further calcinated at 500 ℃ for 3 h in a muffle furnace. Moreover, Hacac, ODE, and ethanol were also recovered during the synthesis of 4.5%-$CuO/ZnO/ZrO_2$ NCs.

10.2 Successive rounds of 4.5%-$CuO/ZnO/ZrO_2$ NCs synthesis with recovered solvents. The recovered solvents were reused for the multi-round fabrication of 4.5%-$CuO/ZnO/ZrO_2$ NCs. $Cu(acac)_2$, $Zn(acac)_2$, and $Zr(acac)_4$ were obtained from the recovered Hacac and supplemented fresh Hacac. The recovered ODE and ethanol still served as the synthesis solvent and precipitating agent, respectively. The amount of recovered Hacac, ODE/OA, and EtOH were firstly detected via GC after each synthesis round. Based on this, corresponding fresh solvents were then supplemented before the next synthesis process. The solvents were recovered and reused four times with the production of five batches of NCs. The amounts of recovered and supplemented solvents during each synthesis round were listed in **Table S4**.

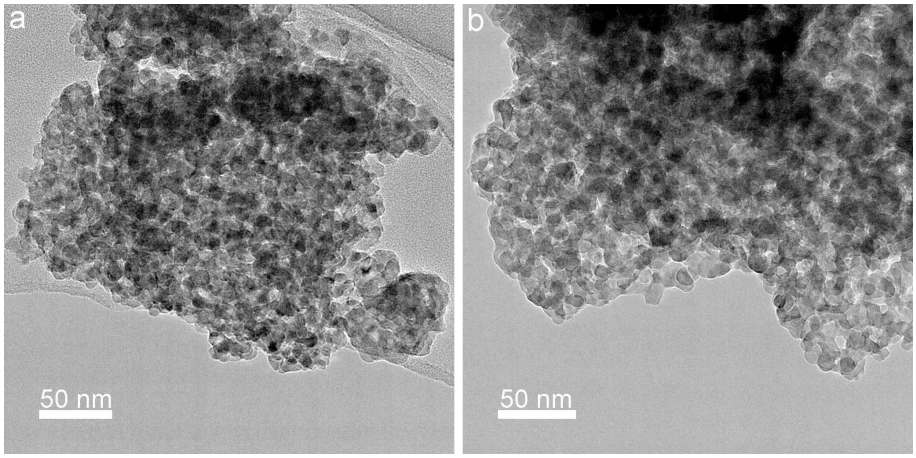

Figure S34. TEM images of 4.5%-CuO/ZnO/ZrO_2 NCs in the first round.

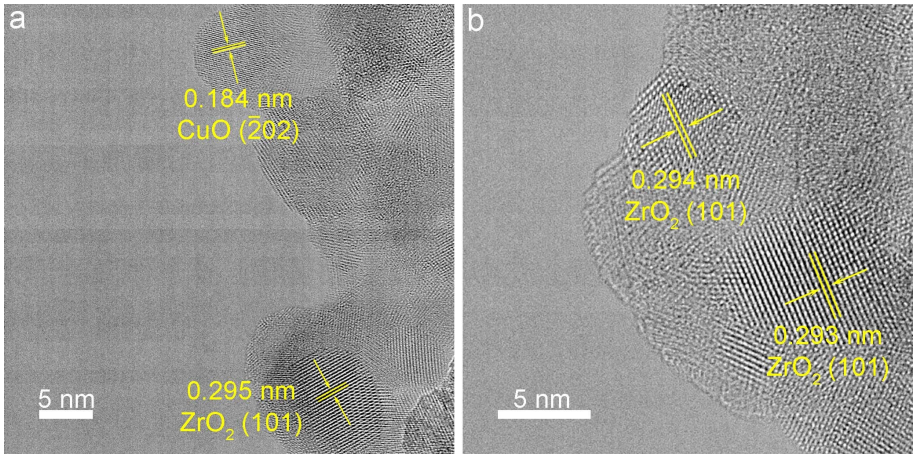

Figure S35. High-resolution TEM images of 4.5%-CuO/ZnO/ZrO_2 NCs.

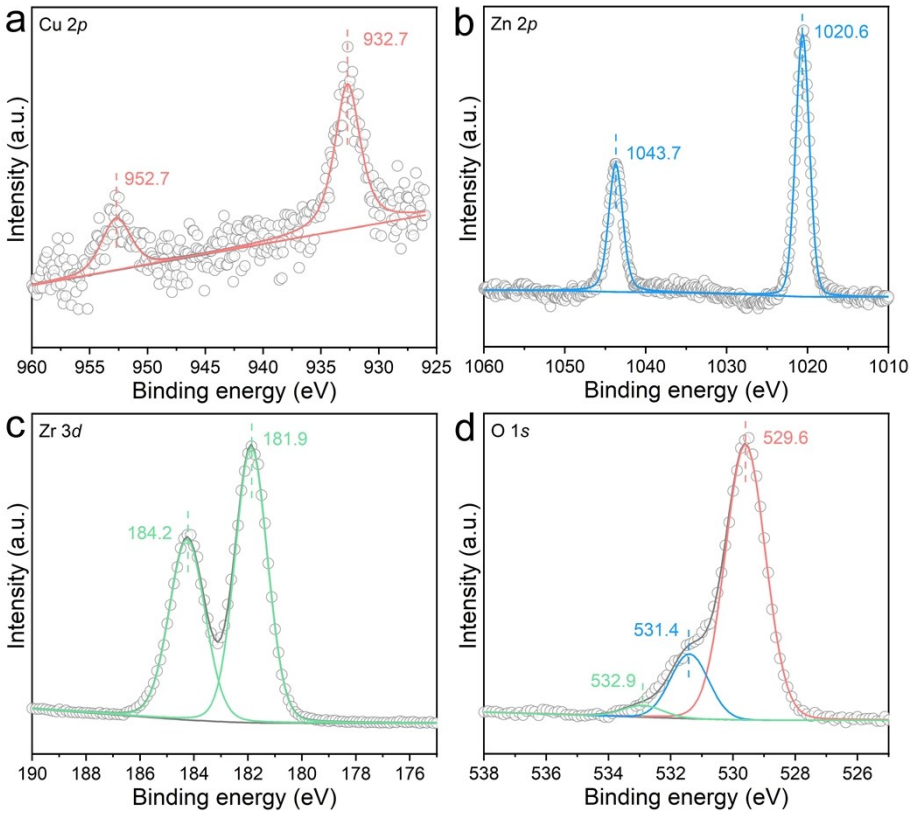

Figure S36. (a) Cu 2*p*, (b) Zn 2*p*, (c) Zr 3*d*, and (d) O 1*s* XPS spectra of 4.5%-CuO/ZnO/ZrO_2 NCs.

Table S4. The amount of recovered and supplemented solvents during each synthesis round.

Round	$V_{solvents}$ (mL)[a]	R_{ODE} (%)[b]	S_{ODE} (mL)[c]	S_{OA} (mL)[d]	R_{EtOH} (%)[e]	S_{EtOH} (mL)[f]
1	124	80.2	16	10	97.5	20
2	148	87.8	0	10	96.5	28
3	140	73.4	0	10	98.4	13
4	130	90.0	10	10	97.3	22
5	145	87.7	/	/	96.6	/

[a] $V_{solvents}$, the overall volume of recovered solvents after rotary evaporation. [b] R_{ODE}, the recovery rate of ODE. [c] S_{ODE}, the volume of supplemented ODE. [d] S_{OA}, the volume of supplemented OA. [e] R_{EtOH}, the recovery rate of ethanol. [f] S_{EtOH}, the volume of supplemented ethanol.

OA as the surfactant was almost completely consumed in each synthesis round. Accordingly, the recovered solvent was directly added 10 mL of fresh OA before the next synthesis round. ODE was supplemented in rounds 1 and 4 to ensure that the whole volume of the reaction solvent remained at 150 mL.

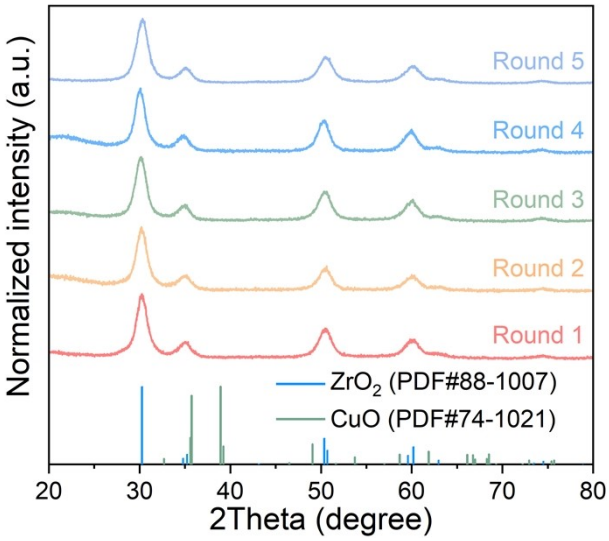

Figure S37. XRD patterns of 4.5%-CuO/ZnO/ZrO_2 NCs for five successive rounds.

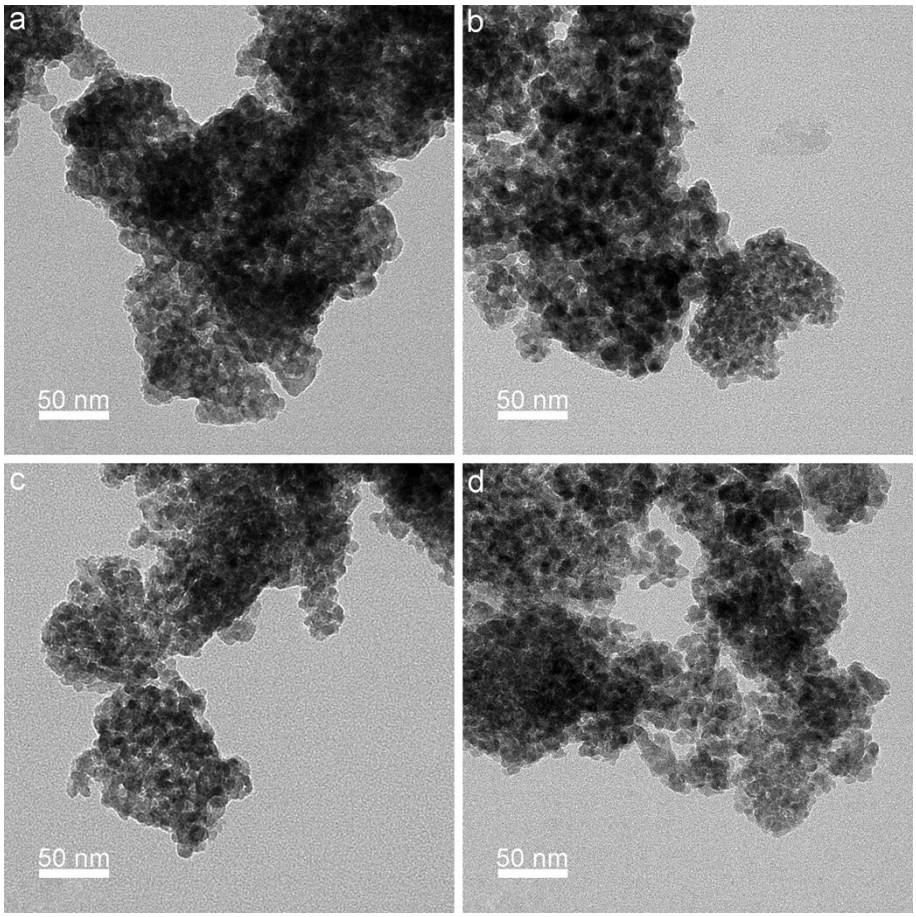

Figure S38. TEM images of 4.5%-CuO/ZnO/ZrO_2 NCs for successive rounds (Rounds 2-5).

Table S5. BET surface areas of 4.5%-CuO/ZnO/ZrO_2 NCs for five successive rounds.

Round	BET surface area (m^2/g)
1	50.3
2	51.4
3	54.4
4	53.4
5	62.7

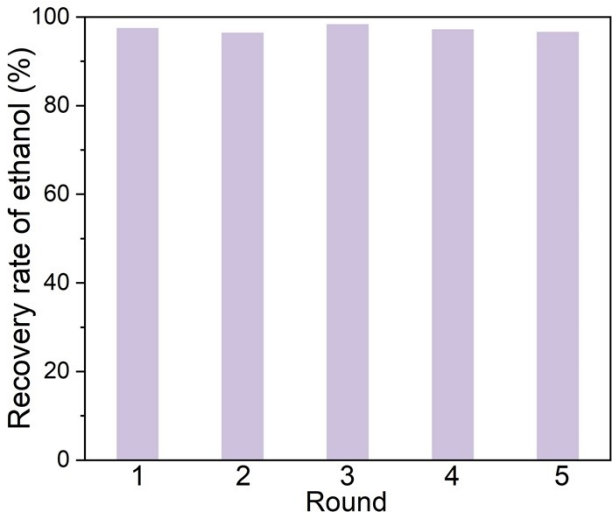

Figure S39. Recovery rates of ethanol during each synthesis round of 4.5%-CuO/ZnO/ZrO_2 NCs.

11. Catalytic CO_2 hydrogenation over CuO/ZnO/ZrO_2 NCs

11.1 Synthesis of CuO/ZnO/ZrO_2 with different CuO molar ratios. CuO/ZnO/ZrO_2 NCs with different CuO molar ratios were prepared following the same method with 4.5%-CuO/ZnO/ZrO_2 NCs except for the regulation of metallic precursors (**Tables S6-S7**).

11.2 Catalytic tests of CuO/ZnO/ZrO_2 NCs in CO_2 hydrogenation. The hydrogenation of CO_2 over CuO/ZnO/ZrO_2 NCs was conducted on a fixed-bed stainless-steel tubular reactor with a quartz tube as the lining (vodo company). In a typical catalytic test, 0.5g of CuO/ZnO/ZrO_2 NCs was diluted with 0.5 g of quartz sand and then packed in the quartz tube. Prior to each catalytic measurement, the catalyst was reduced in H_2/Ar mixed gas flow (H_2/Ar = 1/9, 50 sccm) at 350 °C for 1 h under atmospheric pressure. Then the temperature was cooled down to 40 °C, and the reductive gas was replaced by the reaction gas (H_2/CO_2/N_2 = 72/24/4, N_2 as the internal standard). The standard reaction was conducted at 260 °C under 3.0 MPa with a WHSV of 14400 $mL \cdot g_{cat.}^{-1} \cdot h^{-1}$. The reactants and products flowing out in the reactors were analyzed by an online gas chromatographer (GC, FULI 9790 II) equipped with a thermal conductivity detector (TCD) and a flame ionization detector (FID). The internal standard method was applied to calculate the amounts of products. CO_2 conversion, STY, and selectivity were obtained from the GC data. Besides, the catalytic performance under different temperatures, pressures, and WHSV was also evaluated. Each condition is maintained for 4 h to collect the related data. The CO_2 conversion rate (X_{CO2}), STY, and selectivity of methanol (S_{MeOH}) were defined in the following equations:

$$X_{CO2} = \frac{n_{CO2,in} - n_{CO2,out}}{n_{CO2,in}} \times 100\%$$

$$S_{MeOH} = \frac{n_{MeOH}}{n_{CO2,in} - n_{CO2,out}} \times 100\%$$

$$STY_{(MeOH)}\left(mg_{MeOH} \cdot g_{cat.}^{-1} \cdot h^{-1}\right) = \frac{n_{CO2,in} \times X_{co2} \times S_{MeOH} \times M_{MeOH} \times 1000}{m_{cat.}}$$

where $n_{CO2,out}$ and n_{MeOH} represented the outflow rate of CO_2 and methanol ($mol \cdot h^{-1}$),

respectively; $n_{CO2,in}$ was the inflow rate of CO_2 (mol·h^{-1}); M_{MeOH} and $m_{cat.}$ represented the relative molecular mass of MeOH and the mass of the catalyst (g), respectively.

Table S6. The amount of $M(acac)_x$ used in the synthesis of $CuO/ZnO/ZrO_2$ NCs with different CuO molar ratios.

Sample	$Cu(acac)_2$ (g)	$Zn(acac)_2$ (g)	$Zr(acac)_4$ (g)
ZnO/ZrO_2	/	2.24	27.74
1.8%-$CuO/ZnO/ZrO_2$	0.32	2.22	27.46
8.8%-$CuO/ZnO/ZrO_2$	1.58	2.13	26.35
16.9%-$CuO/ZnO/ZrO_2$	3.15	2.02	24.96

Table S7. Chemical compositions (molar ratios) of $CuO/ZnO/ZrO_2$ NCs determined by ICP-AES.

Sample	Cu (%)	Zn (%)	Zr (%)
ZnO/ZrO_2	/	13.9	86.1
1.8%-$CuO/ZnO/ZrO_2$	1.6	13.1	85.3
4.5%-$CuO/ZnO/ZrO_2$	4.1	13.4	82.7
8.8%-$CuO/ZnO/ZrO_2$	8.5	12.7	78.8
16.9%-$CuO/ZnO/ZrO_2$	15.5	11.3	73.2

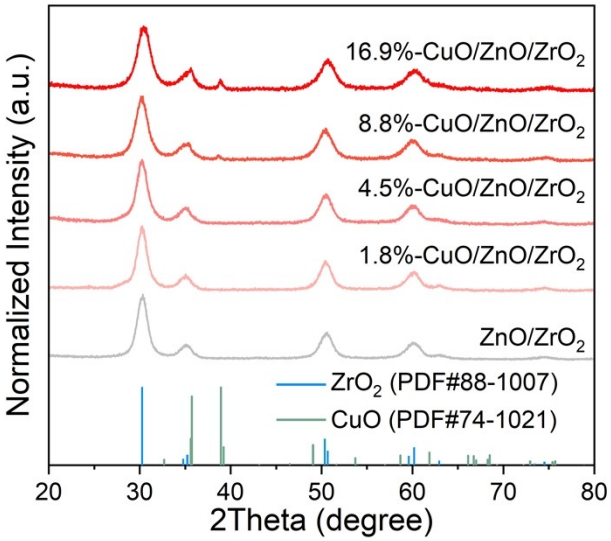

Figure S40. XRD patterns of $CuO/ZnO/ZrO_2$ NCs with different CuO molar ratios.

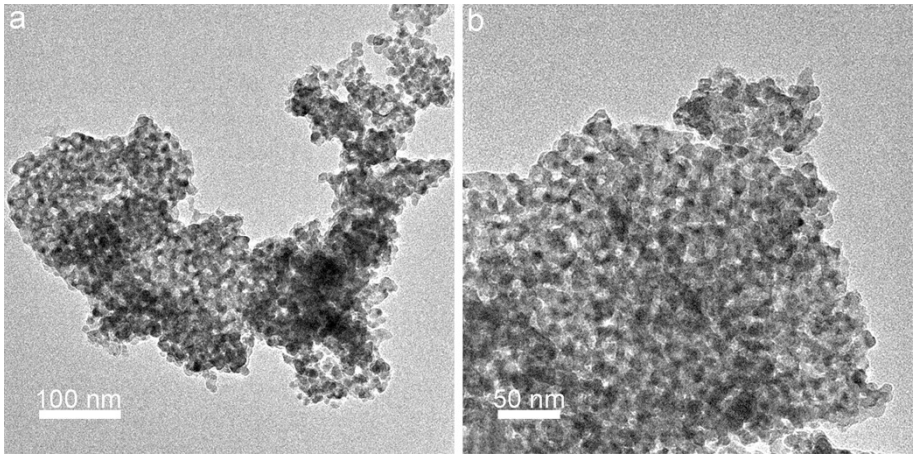

Figure S41. (a-b) TEM images of the pre-reduced 4.5%-CuO/ZnO/ZrO_2 NCs.

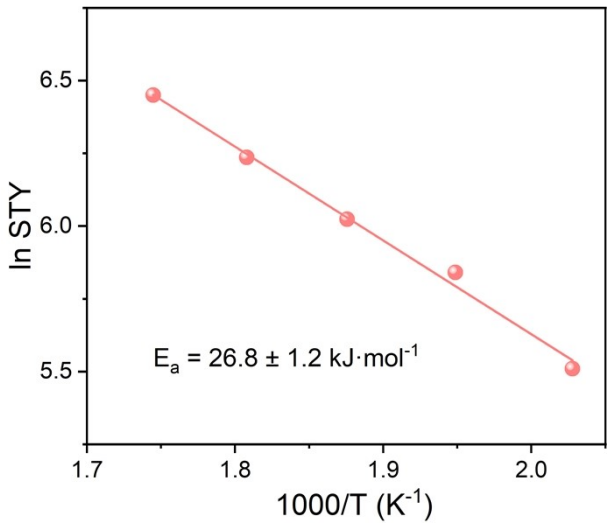

Figure S42. The Arrhenius plot for methanol synthesis over 4.5%-CuO/ZnO/ZrO_2 NCs.

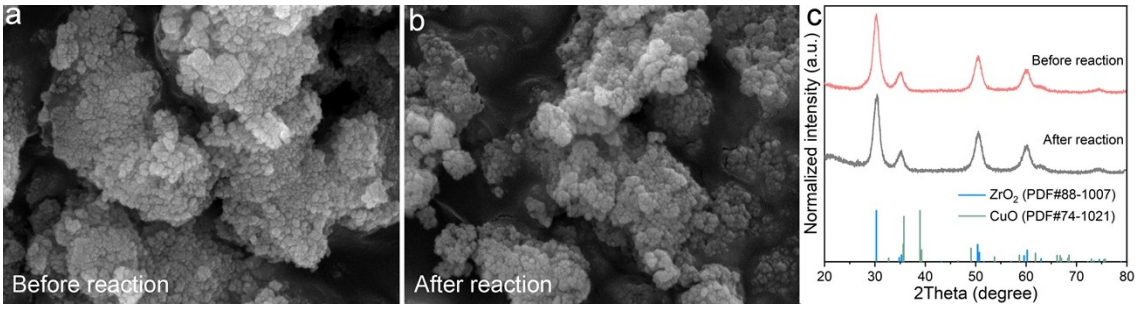

Figure S43. (a and b) SEM images and (c) XRD patters of 4.5%-CuO/ZnO/ZrO_2 NCs before and after the catalytic test.

Table S8. Summary of different catalysts for the hydrogenation CO_2 into methanol in recent literature.

Catalysts	T (°C)	P (MPa)	H_2/CO_2	WHSV[a]	Conv. (%)[b]	Sel. (%)[c]	STY[d]	*Ref.*
4.5%-$CuO/ZnO/ZrO_2$	260	3	3	14400	10.8	77.5	413.0	*This work*
ZnO/ZrO_2	320	5	4	24000	10	91	720	S12
Cu_1/ZrO_2 single-atom catalyst	180	3	3	1200	~1.5	~100	~6.4	S13
$Cu/ZnO/ZrO_2$	220	3	3	6000	18.2	80.6	297	S14
$ZnO/Cu/ZnO/ZrO_2$	277	3	3	7500[e]	6.5	~45%	121.6	S15
$Cu/ZnO/ZrO_2$	250	3	3	3600	17.5	~49	137.6	S16
$Cu/ZnO/ZrO_2$	240	4	3	18000	~15	~80	750	S17
$Cu/ZnO/ZrO_2$	200	2	4	48000	~4	~80	450	S18
$Cu/ZnO/ZrO_2$	250	3	3	24000	9	45	319	S19
$Cu/ZnO/ZrO_2$/GO	240	2	3	15600	~15.5	~35	~280	S20

[a] WHSV, $mL \cdot g_{cat.}^{-1} \cdot h^{-1}$. [b] Conv., the conversion rate of CO_2. [c] Sel., the selectivity of methanol. [d] STY, $mg_{MeOH} \cdot g_{cat.}^{-1} \cdot h^{-1}$. [e] Gas hourly space velocity (GHSV), h^{-1}.

12. Instrumentations

TEM and HAADF-STEM images for 4.5%-CuO/ZnO/ZrO_2 NCs in the first round were collected on a JEOL ARM200F field-emission transmission electron microscope with an acceleration voltage of 200 kV. Other TEM images were collected on a transmission electron microscope (Talos F200X). The morphology features of 4.5%-CuO/ZnO/ZrO_2 NCs-used were obtained SEM (Quanta FEG 250). XRD patterns were recorded using the Rigaku X-ray diffractometer (Rigaku, MiniFlex 600) with Cu-Kα radiation (λ = 1.54178 Å). XPS measurements were operated in Kratos Axis supra+. All of the XPS data were fitted by "XPS Peak Fitting Program for WIN95/98 XPSPEAK Version 4.1" developed by Raymund W.M. Kwok. The amount of water in ODE was determined by Kulun Carl Fischer moisture meter (Metrohm-852). FTIR spectroscopy was carried out with a FTIR spectrometer (Bruker TENSOR II). The BET surface areas of the samples were measured on a Micromeritics ASAP 2460 adsorption apparatus. ICP-AES (Atomscan Advantage, Thermo Jarrell Ash, USA) was used to determine the molar ratios of Cu, Zn, and Zr in CuO/ZnO/ZrO_2 NCs.

References

S1. S. Yoda, Y. Takebayashi, K. Sue, T. Furuya and K. Otake, *J. Supercrit. Fluids*, 2017, **123**, 82-91.

S2. N. V. Belova, H. Oberhammer, N. H. Trang and G. V. Girichev, *J. Org. Chem.*, 2014, **79**, 5412-5419.

S3. O. Chen, X. Chen, Y. Yang, J. Lynch, H. Wu, J. Zhuang and Y. C. Cao, *Angew. Chem. Int. Ed.*, 2008, **47**, 8638-8641.

S4. J. Park, K. An, Y. Hwang, J. G. Park, H. J. Noh, J. Y. Kim, J. H. Park, N. M. Hwang and T. Hyeon, *Nat. Mater.*, 2004, **3**, 891-895.

S5. S. Lee, J.-S. Yoon, S. Kang, K. Kwon, K. S. Chang, S. Lee, S.-I. Choi, J.-R. Jeong, G. Lee, K. M. Nam and P. Davies, *J. Am. Ceram. Soc.*, 2016, **99**, 2578-2584.

S6. X. Guo, W. Wang, Y. Yang and Q. Tian, *CrystEngComm*, 2016, **18**, 9033-9041.

S7. M. Park, N. Lee, S. H. Choi, K. An, S.-H. Yu, J. H. Kim, S.-H. Kwon, D. Kim, H. Kim, S.-I. Baek, T.-Y. Ahn, O. K. Park, J. S. Son, Y.-E. Sung, Y.-W. Kim, Z. Wang, N. Pinna and T. Hyeon, *Chem. Mater.*, 2011, **23**, 3318-3324.

S8. S. H. Choi, E. G. Kim, J. Park, K. An, N. Lee, S. C. Kim and T. Hyeon, *J. Phys. Chem. B*, 2005, **109**, 14792-14794.

S9. G. Garnweitner, L. M. Goldenberg, O. V. Sakhno, M. Antonietti, M. Niederberger and J. Stumpe, *Small*, 2007, **3**, 1626-1632.

S10. T. Yu, Y. I. Park, M.-C. Kang, J. Joo, J. K. Park, H. Y. Won, J. J. Kim and T. Hyeon, *Eur. J. Inorg. Chem.*, 2008, DOI: 10.1002/ejic.200700979, 855-858.

S11. T. Y. Yu, J. Joo, Y. I. Park and T. Hyeon, *Angew. Chem. Int. Ed.*, 2005, **44**, 7411-7414.

S12. J. Wang, G. Li, Z. Li, C. Tang, Z. Feng, H. An, H. Liu, T. Liu and C. Li, *Sci. Adv.*, 2017, **3**, e1701290.

S13. H. Zhao, R. Yu, S. Ma, K. Xu, Y. Chen, K. Jiang, Y. Fang, C. Zhu, X. Liu, Y. Tang, L. Wu, Y. Wu, Q. Jiang, P. He, Z. Liu and L. Tan, *Nat. Catal.*, 2022, **5**, 818-831.

S14. W. Yuhao, K. Shyam, G. Wengui, L. Kongzhai, L. Ping, G. C. Jingguang and W. Hua, *Nat.*

Commun., 2019, **10**, 1166.

S15. A. Arandia, J. Yim, H. Warraich, E. Leppakangas, R. Bes, A. Lempelto, L. Gell, H. Jiang, K. Meinander, T. Viinikainen, S. Huotari, K. Honkala and R. L. Puurunen, *Appl. Catal. B*, 2023, **321**, 122046.

S16. H. Chen, H. Cui, Y. Lv, P. Liu, F. Hao, W. Xiong and H. a. Luo, *Fuel*, 2022, **314**, 123035.

S17. Y. Wang, W. Gao, K. Li, Y. Zheng, Z. Xie, W. Na, J. G. Chen and H. Wang, *Chem*, 2020, **6**, 419-430.

S18. T. Zou, T. P. Araujo, F. Krumeich, C. Mondelli and J. Perez-Ramirez, *ACS Sustain. Chem. Eng.*, 2022, **10**, 81-90.

S19. F. C. F. Marcos, L. Lin, L. E. Betancourt, S. D. Senanayake, J. A. Rodriguez, J. M. Assaf, R. Giudici and E. M. Assaf, *J. CO_2 Util.*, 2020, **41**, 101215.

S20. T. Witoon, T. Numpilai, T. Phongamwong, W. Donphai, C. Boonyuen, C. Warakulwit, M. Chareonpanich and J. Limtrakul, *Chem. Eng. J.*, 2018, **334**, 1781-1791.